into PrE cells would promote ExEn differentiation. Therefore, we examined the stage-specific role of SOX17 in ExEn differentiation. Ad-SOX17 transduction was performed in human ESCs treated with BMP4 for 0, 1, 2, 3, or 4 days, and the Ad-SOX17-transduced cells were cultured with medium containing BMP4 until day 5 (Figures 1A–1D). We confirmed the expression of exogenous SOX17 in the human ESC-derived mesendoderm cells transduced with Ad-SOX17 (Figure S3). Since BMP4 is known for its capability to induce both ExEn and trophectoderm [8,9], we analyzed not only the expression levels of ExEn markers but also those of trophectoderm markers by real-time RT-PCR after 5 days of differentiation (Figures 1A and 1B). The transduction of Ad-SOX17 on day 1 led to the highest expression levels of ExEn markers, alpha-fetoprotein (AFP), GATA4, laminin B1 (LAMB1), and SOX7 [17,18,19]. In contrast, the expression levels of the trophectoderm markers CDX2, GATA2, hCGα (human chorionic gonadotropin), and hCGβ [20] were down-regulated in Ad-SOX17-transduced cells as compared with non-transduced cells (Figure 1B). The expression levels of the pluripotent marker NANOG and DE marker GSC were not increased by SOX17 transduction (Figures 1C and 1D). We confirmed that there were no differences between non-transduced cells and Ad-LacZ-transduced cells in gene expression levels of all the markers investigated in Figures 1A–1D (data not shown). Therefore, we concluded that ExEn cells were efficiently induced from Ad-SOX17-transduced PrE cells.

The effects of SOX17 transduction on the ExEn differentiation from human ESC-derived PrE cells were also assessed by quantifying AFP- or SOX7-positive ExEn cells. The percentage of AFP- or SOX7-positive cells was significantly increased in Ad-SOX17-transduced cells (69.7% and 63.3%, respectively) (Figure 1E). Similar results were observed in the human iPS cell lines (201B7, Dotcom, and Tic) (Figure 1F). These findings indicated that stage-specific SOX17 overexpression in human ESC-derived PrE cells enhances ExEn differentiation.

Mesendoderm stage-specific SOX17 overexpression promotes directive DE differentiation from human ESCs

To examine the effects of transient SOX17 overexpression on DE differentiation from human ESCs, we optimized the timing of the Ad-SOX17 transduction. Ad-SOX17 transduction was performed in human ESCs treated with Activin A (100 ng/ml) for 0, 1, 2, 3, or 4 days, and the Ad-SOX17-transduced cells were cultured with medium containing Activin A (100 ng/ml) until day 5 (Figures 2A–2C). Using a fiber-modified Ad vector, both undifferentiated human ESCs and Activin A-induced human ESC-derived cells were efficiently transduced (Figure S4). The transduction of SOX17 on day 3 led to the highest expression levels of the DE markers FOXA2 [21], GSC [22], GATA4 [17], and HEX [23] (Figure 2A). In contrast to the DE markers, the expression levels of the pluripotent marker NANOG [24] were down-regulated in Ad-SOX17-transduced cells as compared with non-transduced cells (Figure 2B). The expression levels of the ExEn marker SOX7 [14] were up-regulated, when Ad-SOX17 transduction was performed into human ESCs treated with Activin A (100 ng/ml) for 0, 1, or 2 days (Figure 2C). On the other hand, the expression levels of the ExEn marker SOX7 were significantly down-regulated, when Ad-SOX17 transduction was performed into human ESCs treated with Activin A (100 ng/ml) for 3 or 4 days, indicating that SOX17 overexpression prior to mesendoderm formation (day 0, 1, and 2) promoted not only DE differentiation but also ExEn differentiation. Similar results were obtained with the human iPS cell line (Tic) (Figure S5). Although the expression levels of the mesoderm marker FLK1 [25] did not exhibit any change when Ad-SOX17 transduction was performed into human ESCs treated with Activin A (100 ng/ml) for 0, 1, or 2 days (Figure 2D), their expression levels were significantly down-regulated when Ad-SOX17 transduction was performed into human ESCs treated with Activin A (100 ng/ml) for 3 or 4 days. These results suggest that SOX17 overexpression promotes directive differentiation from mesendoderm cells into the DE cells, but not into mesoderm cells. We also confirmed that Ad-vector mediated gene expression in the human ESC-derived mesendoderm cells (day 3) continued until day 6 and disappeared on day 10 (Figure S6). SOX17 transduction in the human ESC-derived cells on day 3 and 4 had no effect on cell viability, while that in the cells on day 0, 1, and 2 resulted in severely impaired cell viability (Figure S7), probably because SOX17 transduction directed the cells on day 0, 1, and 2 to differentiate into ExEn cells but the medium containing Activin A (100 ng/ml) was inappropriate for ExEn cells. We confirmed that there were no differences between non-transduced cells and Ad-LacZ-transduced cells in gene expression levels of all the markers investigated in Figures 2A–2D (data not shown). These results indicated that stage-specific SOX17 overexpression in human ESC-derived mesendoderm cells is essential for promoting efficient DE differentiation.

It has been previously reported that human ESC-derived mesendoderm cells and DE cells became CXCR4-positive (>80%) by culturing human ESCs with Activin A (100 ng/ml) [26]. However, Activin A is not sufficient for homogenous differentiation of c-Kit/CXCR4-double-positive DE cells [10,11] or HEX-positive anterior DE cells [23]. Seguin et al. and Morrison et al. reported that the differentiation efficiency of c-Kit/CXCR4-double-positive DE cells was approximately 30% in the absence of stable Sox17 expression and that of HEX-positive anterior DE cells was only about 10% [10,23]. Therefore, we next examined whether Ad-SOX17 transduction improves the differentiation efficiency of c-Kit/CXCR4-double-positive DE cells and HEX-positive anterior DE cells. Human ESC-derived mesendoderm cells were transduced with Ad-SOX17, and the number of CXCR4/c-Kit-double-positive cells was analyzed by using a flow cytometer. The percentage of CXCR4/c-Kit-double-positive cells was significantly increased in Ad-SOX17-transduced cells (67.7%), while that in Ad-LacZ-transduced cells was only 22% (Figure 2E). The percentage of HEX-positive cells was also significantly increased in Ad-SOX17-transduced cells (53.7%), while that in Ad-LacZ-transduced cells was approximately 11% (Figure 2F). Similar results were also observed in the three human iPS cell lines (201B7, Dotcom, and Tic) (Figure 2G). These findings indicated that stage-specific SOX17 overexpression in human ESC-derived mesendoderm cells promotes efficient differentiation of DE cells.

Ad-SOX17-transduced cells tend to differentiate into the hepatic lineage

To investigate whether Ad-SOX17-transduced cells have the ability to differentiate into hepatoblasts and hepatocyte-like cells, Ad-SOX17-transduced cells were differentiated according to our previously described method [13]. Our previous report demonstrated that transient HEX transduction efficiently generates hepatoblasts from human ESC- and iPSC-derived DE cells. The hepatic differentiation protocol used in this study is illustrated in Figure 3A. After the hepatic differentiation, the morphology of human ESCs transduced with Ad-SOX17 followed by Ad-HEX was gradually changed into a hepatocyte morphology: polygonal in shape with distinct round nuclei by day 18 (Figure 3B). We also

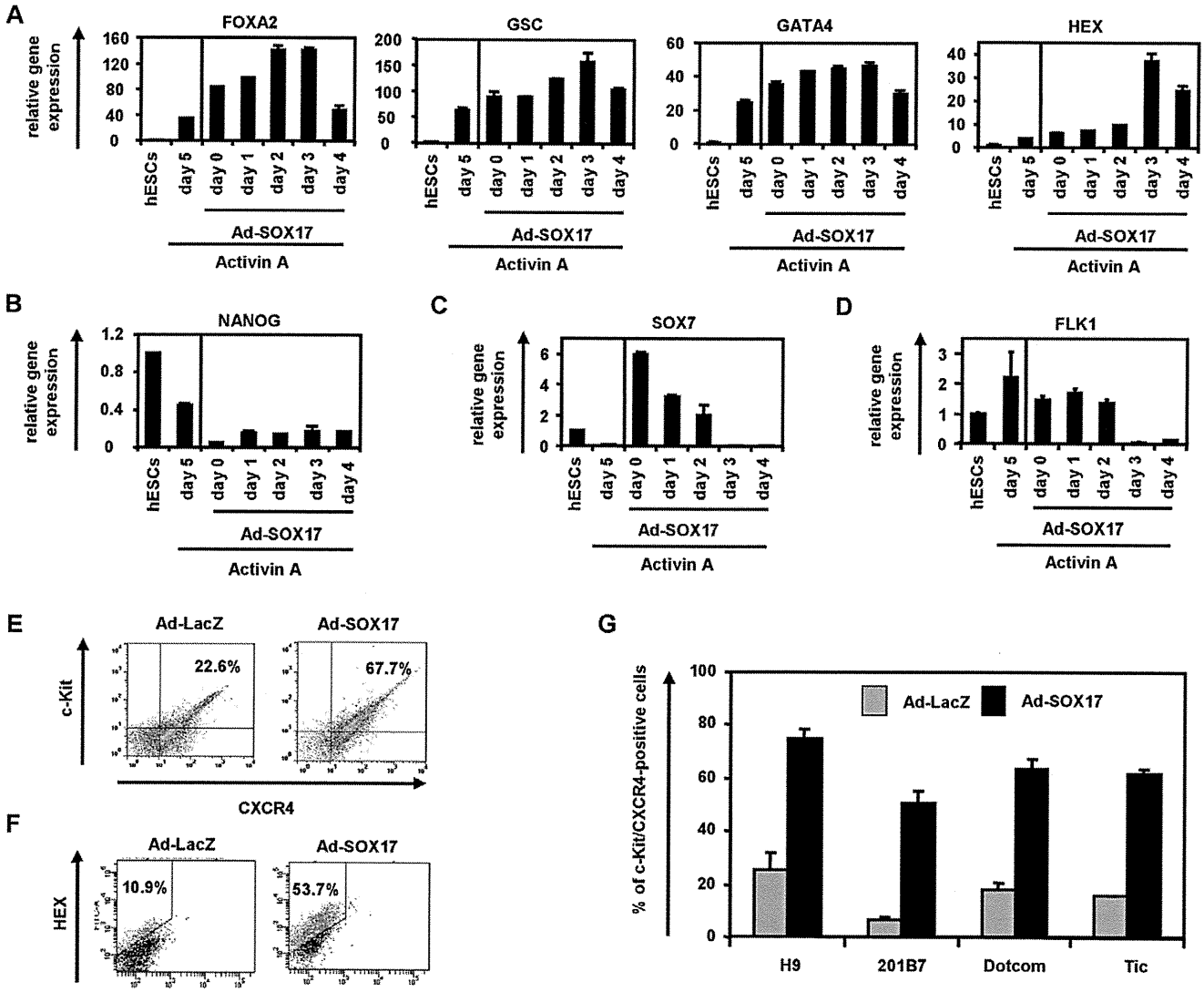

Figure 2. Efficient DE differentiation from human ESC- and iPSC-derived mesendoderm cells by SOX17 transduction. (A–D) Undifferentiated human ESCs (H9) and Activin A-induced human ESC-derived cells, which were cultured with the medium containing Activin A (100 ng/ml) for 0, 1, 2, 3, and 4 days, were transduced with 3,000 VP/cell of Ad-SOX17 for 1.5 h. Ad-SOX17-transduced cells were cultured with 100 ng/ml of Activin A, and the gene expression levels of (A) the DE markers (FOXA2, GSC, and GATA4) and anterior DE marker (HEX), (B) the pluripotent marker (NANOG), (C) the ExEn marker (SOX7), and (D) the mesoderm marker (FLK1) were examined by real-time RT-PCR on day 5 of differentiation. The horizontal axis represents the day on which the cells were transduced with Ad-SOX17. The expression levels of human ESCs on day 0 were defined 1.0. (E, F) After human ESCs were cultured with 100 ng/ml of Activin A for 3 days, human ESC-derived mesendoderm cells were transduced with Ad-LacZ or Ad-SOX17 and cultured until day 5. Ad-LacZ- or Ad-SOX17-transduced DE cells were subjected to immunostaining with anti-c-Kit, anti-CXCR4 (E) and anti-HEX antibodies (F) and then analyzed by flow cytometry. (G) After Ad-LacZ or Ad-SOX17 transduction, the DE differentiation efficacies of the human ES cell line (H9) and three human iPS cell lines (201B7, Dotcom, and Tic) were compared at day 5 of differentiation. All data are represented as the means±SD ($n = 3$).
doi:10.1371/journal.pone.0021780.g002

examined hepatic gene and protein expression levels on day18 of differentiation. For this purpose, we used a human ES cell line (H9) and three human iPS cell lines (201B7, Dotcom, Tic). On day 18 of differentiation, the gene and protein expression analysis showed up-regulation of the hepatic markers albumin (ALB) [27], cytochrome P450 2D6 (CYP2D6), CYP3A4, and CYP7A1 [28] mRNA and ALB, CYP2D6, CYP3A4, CYP7A1, and cytokeratin (CK)18 proteins in both Ad-SOX17- and Ad-HEX-transduced cells transduced cells as compared with both Ad-LacZ- and Ad-HEX-transduced cells (Figures 4A and 4B). These results indicated that Ad-SOX17-transduced cells were more committed to the hepatic lineage than non-transduced cells.

Discussion

The directed differentiation from human ESCs and iPSCs is a useful model system for studying mammalian development as well as a powerful tool for regenerative medicine [29]. In the present study, we elucidated the bidirectional role of SOX17 on either ExEn or DE differentiation from human ESCs and iPSCs. We initially confirmed that initiation of SOX17 expression was consistent with the time period of PrE or mesendoderm cells formation (Figures S1 and S2). We speculated that stage-specific transient SOX17 transduction in PrE or mesendoderm could enhance ExEn or DE differentiation from human ESCs and iPSCs, respectively.

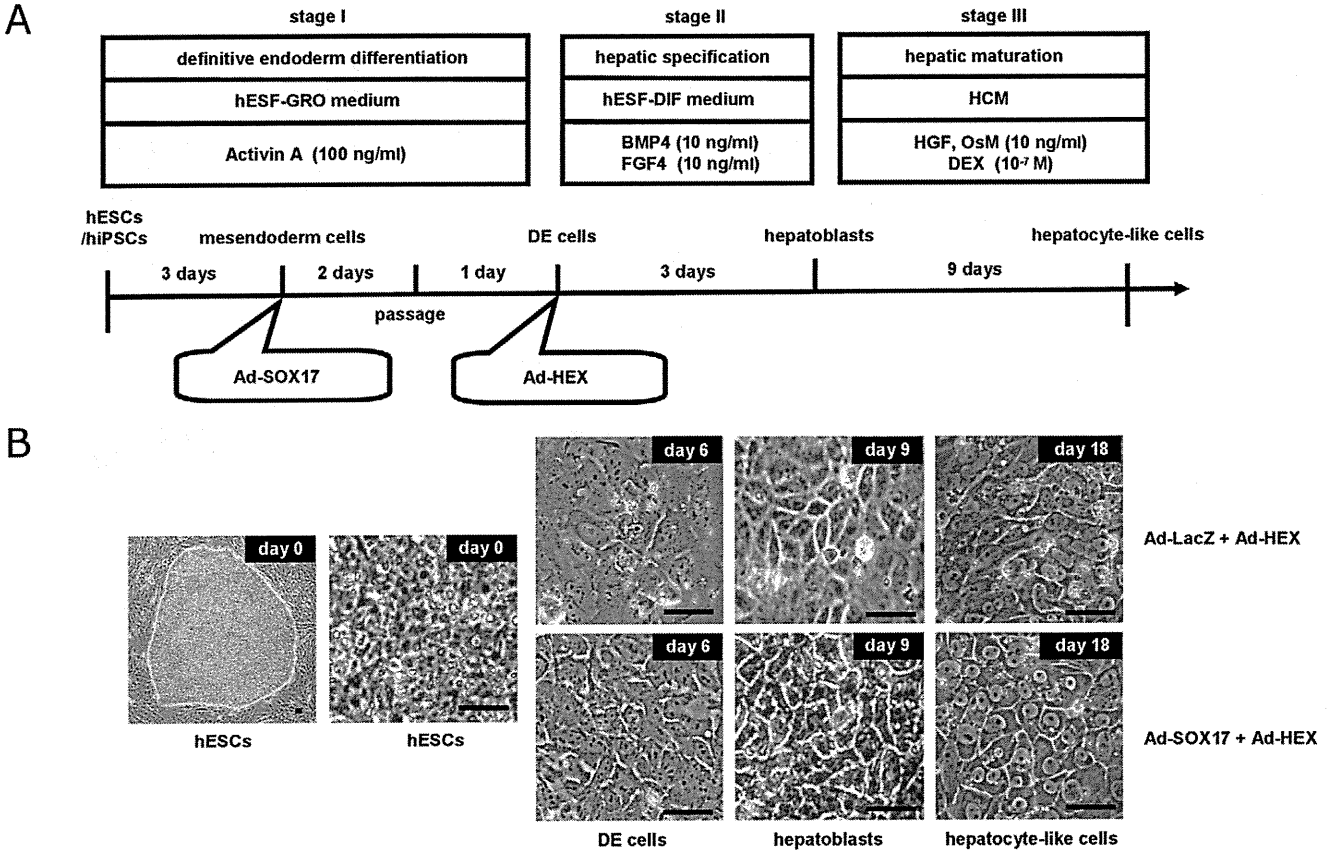

Figure 3. Hepatic Differentiation of Human ESC- and iPSC-Derived DE Cells Transduced with Ad-HEX. (A) The procedure for differentiation of human ESCs and iPSCs into hepatoblasts and hepatocyte-like cells is presented schematically. Both hESF-GRO and hESF-DIF medium were supplemented with 5 factors and 0.5 mg/ml fatty acid-free BSA, as described in the Materials and Methods section. (B) Sequential morphological changes (day 0–18) of human ESCs (H9) differentiated into hepatocyte-like cells via the DE cells and the hepatoblasts are shown. The scale bar represents 50 μm.
doi:10.1371/journal.pone.0021780.g003

SOX17 transduction at the pluripotent stage promoted random differentiation giving heterogeneous populations containing both ExEn and DE cells were obtained (Figures 2A–2C). Qu et al. reported that SOX17 promotes random differentiation of mouse ESCs into PrE cells and DE cells *in vitro* [30], which is in consistent with the present study. Previously, Niakan et al. and Seguin et al. respectively demonstrated that ESCs could promote either ExEn or DE differentiation by stable SOX17 expression, respectively [10,12]. Although these discrepancies might be attributable to differences in the species used in the experiments (i.e., human versus mice), SOX17 might have distinct functions according to the appropriate differentiation stage. To elucidate these discrepancies, we examined the stage-specific roles of SOX17 in the present study, and found that human ESCs and iPSCs could differentiate into either ExEn or DE cells when SOX17 was overexpressed at the PrE or mesendoderm stage, respectively, but not when it was overexpressed at the pluripotent stage (Figures 1 and 2). This is because endogenous SOX17 is strongly expressed in the PrE and primitive streak tissues but only slightly expressed in the inner cell mass, our system might adequately reflect the early embryogenesis [14,31].

In ExEn differentiation from human ESCs, stage-specific SOX17 overexpression in human ESC-derived PrE cells promoted efficient ExEn differentiation and repressed trophectoderm differentiation (Figures 1A and 1B), although SOX17 transduction at the pluripotent stage did not induce the efficient differentiation of ExEn cells. In our protocol, the stage-specific overexpression of SOX17 could elevate the efficacy of AFP-positive or SOX7-positive ExEn differentiation from human ESCs and iPSCs. The reason for the efficient ExEn differentiation by SOX17 transduction might be due to the fact that SOX17 lies downstream from GATA6 and directly regulates the expression of GATA4 and GATA6 [12]. Although it was previously been reported that Sox17 plays a substantial role in late-stage differentiation of ExEn cells *in vitro* [32], those reports utilized embryoid body formation, in which other types of cells, including endoderm, mesoderm, and ectoderm cells, might have influences on cellular differentiation. The present study showed the role of SOX17 in a homogeneous differentiation system by utilizing a mono-layer culture system.

In DE differentiation from human ESCs, we found that DE cells were efficiently differentiated from the human ESC-derived mesendoderm cells by stage-specific SOX17 overexpression (Figure 2). Therefore, we concluded that SOX17 plays a significant role in the differentiation of mesendoderm cells to DE cells. Although SOX17 overexpression before the formation of mesendoderm cells did not affect mesoderm differentiation, SOX17 transduction at the mesendoderm stage selectively promoted DE differentiation and repressed mesoderm differentiation (Figures 2A and 2D). These results show that SOX17 plays a crucial role in decision of DE differentiation from mesendoderm cells, as previous studies suggested [33,34]. Interestingly, SOX17 transduction at the pluripotent stage promoted not only DE

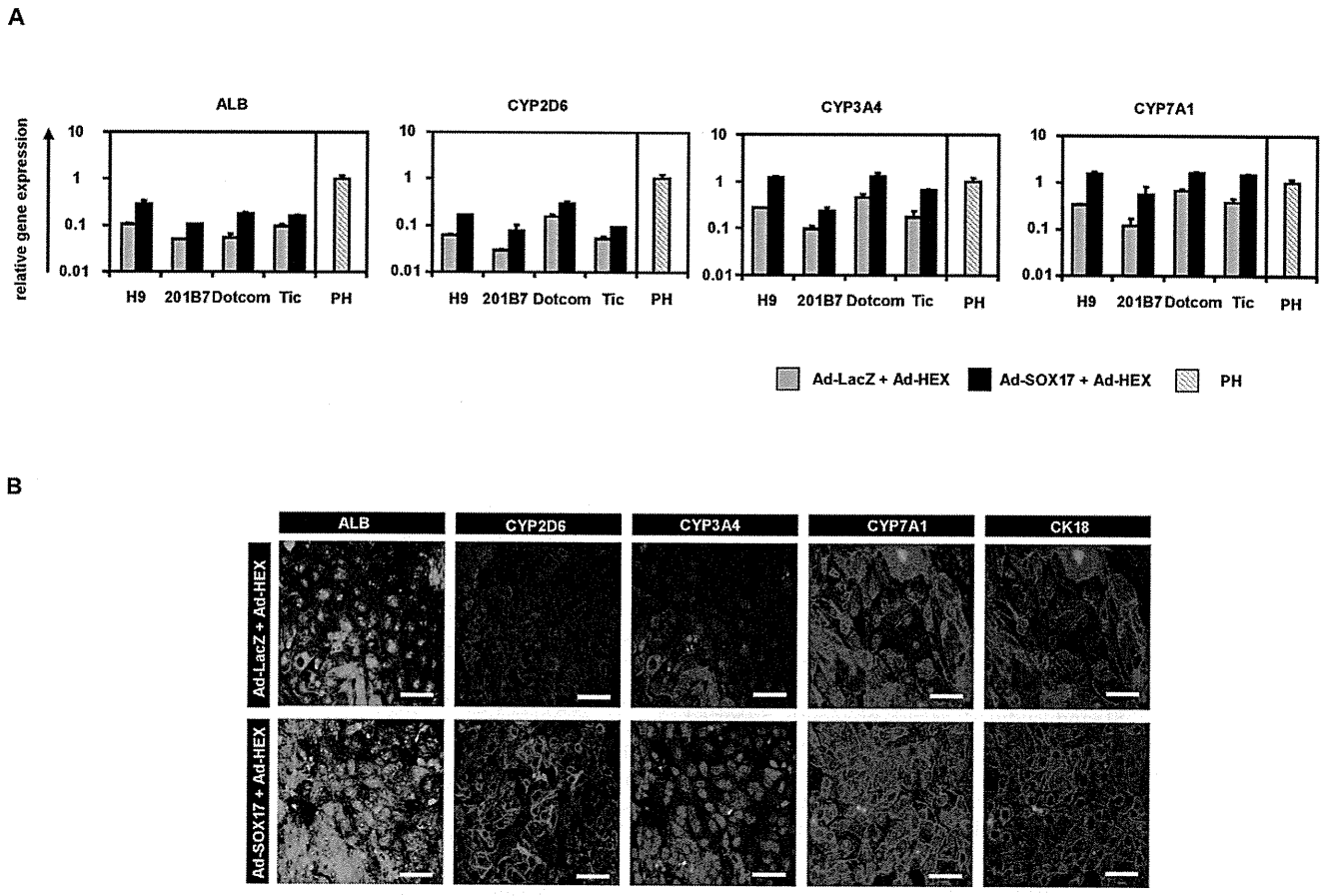

Figure 4. Characterization of hepatocyte-like cells from human ESC- and iPSC-derived DE cells. (A) The Ad-LacZ-transduced cells and Ad-SOX17-transduced cells were transduced with 3,000 VP/cell of Ad-HEX for 1.5 h on day 6. On day 18 of differentiation, the levels of expression of the hepatocyte markers (ALB, CYP2D6, CYP3A4, and CYP7A1) were examined by real-time RT-PCR in human ESC (H9)-derived hepatocyte-like cells and human iPSC (201B7, Dotcom, or Tic)-derived hepatocyte-like cells. The gene expression profiles of cells transduced with both Ad-SOX17 and Ad-HEX (black bar) were compared with those of cells transduced with both Ad-LacZ and Ad-HEX (gray bar). The expression level of primary human hepatocytes (PH, hatched bar), which were cultured 48 h after plating the cells, were defined as 1.0. All data are represented as the means±SD ($n = 3$). (B) The expression of the hepatocyte markers ALB (green), CYP2D6 (red), CYP3A4 (red), CYP7A1 (red), and CK18 (green) was also examined by immunohistochemistry on day 18 of differentiation. Nuclei were counterstained with DAPI (blue). The scale bar represents 50 μm.
doi:10.1371/journal.pone.0021780.g004

differentiation but also ExEn differentiation even in the presence of Activin A (Figures 2A and 2C), demonstrating that transduction at an inappropriate stage of differentiation prevents directed differentiation. These results suggest that stage-specific SOX17 transduction mimicking the gene expression pattern in embryogenesis could selectively promote DE differentiation.

Another important finding about DE differentiation is that the protocol in the present study was sufficient for nearly homogeneous DE and anterior DE differentiation by mesendoderm stage-specific SOX17 overexpression; the differentiation efficacies of c-Kit/CXCR4-double-positive DE cells and HEX-positive anterior DE cells were approximately 70% and 54%, respectively (Figures 2E and 2F). The conventional differentiation protocols without gene transfer were not sufficient for homogenous DE and anterior DE differentiation; the differentiation efficacies of DE and anterior DE were approximately 30% and 10%, respectively [10,11,23]. One of the reasons for the efficient DE differentiation by SOX17 transduction might be the activation of the FOXA2 gene which could regulate many endoderm-associated genes [35]. Moreover, SOX17-transduced cells were more committed to the hepatic lineage (Figure 4). This might be because the number of HEX-positive anterior DE cell populations was increased by SOX17 transduction. Recent studies have shown that the conditional expression of Sox17 in the pancreas at E12.5, when it is not normally expressed, is sufficient to promote biliary differentiation at the expense of endocrine cells [36]. Therefore, we reconfirmed that our protocol in which SOX17 was transiently transduced at the appropriate stage of differentiation was useful for DE and hepatic differentiation from human ESCs and iPSCs.

Using human iPSCs as well as human ESCs, we confirmed that stage-specific overexpression of SOX17 could promote directive differentiation of either ExEn or DE cells (Figures 1F, 2G, and 4A). Interestingly, a difference of DE and hepatic differentiation efficacy among human iPS cell lines was observed (Figures 1F and 2G). Therefore, it would be necessary to select a human iPS cell line that is suitable for hepatic differentiation in the case of medical applications, such as liver transplantation.

To control cellular differentiation mimicking embryogenesis, we employed Ad vectors, which are one of the most efficient transient gene delivery vehicles and have been widely used in both experimental studies and clinical trials [37]. Recently, we have also demonstrated that ectopic HEX expression by Ad vectors in human ESC-derived DE cells markedly enhances the hepatic differentiation [13]. Thus, Ad vector-mediated transient gene

transfer should be a powerful tool for regulating cellular differentiation.

In summary, the findings presented here demonstrate a stage-specific role of SOX17 in the ExEn and DE differentiation from human ESCs and iPSCs (Figure S8). Although previous reports showed that SOX17 overexpression in ESCs leads to differentiation of either ExEn or DE cells, we established a novel method to promote directive differentiation by SOX17 transduction. Because we utilized a stage-specific overexpression system, our findings provide further evidence that the lineage commitment in this method seems to reflects what is observed in embryonic development. In the present study, both human ESCs and iPSCs (3 lines) were used and all cell lines showed efficient ExEn or DE differentiation, indicating that our novel protocol is a powerful tool for efficient and cell line-independent endoderm differentiation. Moreover, the establishing methods for efficient hepatic differentiation by sequential SOX17 and HEX transduction would be useful for *in vitro* applications such as screening of pharmacological compounds as well as for regenerative therapy.

Materials and Methods

In vitro Differentiation

Before the initiation of cellular differentiation, the medium of human ESCs and iPSCs was exchanged for a defined serum-free medium hESF9 [38] and cultured as we previously reported. hESF9 consists of hESF-GRO medium (Cell Science & Technology Institute) supplemented with 5 factors (10 μg/ml human recombinant insulin, 5 μg/ml human apotransferrin, 10 μM 2-mercaptoethanol, 10 μM ethanolamine, and 10 μM sodium selenite), oleic acid conjugated with fatty acid free bovine albumin, 10 ng/ml FGF2, and 100 ng/ml heparin (all from Sigma).

To induce, ExEn cells, human ESCs and iPSCs were cultured for 5 days on a gelatin-coated plate in mouse embryonic conditioned-medium supplemented with 20 ng/ml BMP4 (R&D system) and 1% FCS (GIBCO-BRL).

The differentiation protocol for induction of DE cells, hepatoblasts, and hepatocyte-like cells was based on our previous report with some modifications [13]. Briefly, in DE differentiation, human ESCs and iPSCs were cultured for 5 days on a Matrigel (BD)-coated plate in hESF-DIF medium (Cell Science & Technology Institute) supplemented with the above-described 5 factors, 0.5 mg/ml BSA, and 100 ng/ml Activin A (R&D Systems). For induction of hepatoblasts, the DE cells were transduced with 3,000 VP/cell of Ad-HEX for 1.5 h and cultured in hESF-DIF (Cell Science & Technology Institute) medium supplemented with the above-described 5 factors, 0.5 mg/ml BSA, 10 ng/ml bone morphology protein 4 (BMP4) (R&D Systems), and 10 ng/ml FGF4 (R&D systems). In hepatic differentiation, the cells were cultured in hepatocyte culture medium (HCM) supplemented with SingleQuots (Lonza), 10 ng/ml hepatocyte growth factor (HGF) (R&D Systems), 10 ng/ml Oncostatin M (OsM) (R&D Systems), and 10^{-7} M dexamethasone (DEX) (Sigma).

Human ESC and iPSC Culture

A human ES cell line, H9 (WiCell Research Institute), was maintained on a feeder layer of mitomycin C-treated mouse embryonic fibroblasts (Millipore) with Repro Stem (Repro CELL), supplemented with 5 ng/ml fibroblast growth factor 2 (FGF2) (Sigma). Human ESCs were dissociated with 0.1 mg/ml dispase (Roche Diagnostics) into small clumps, and subcultured every 4 or 5 days. Two human iPS cell lines generated from the human embryonic lung fibroblast cell line MCR5 were provided from the JCRB Cell Bank (Tic, JCRB Number: JCRB1331; and Dotcom, JCRB Number: JCRB1327) [39,40]. These human iPS cell lines were maintained on a feeder layer of mitomycin C-treated mouse embryonic fibroblasts with iPSellon (Cardio), supplemented with 10 ng /ml FGF2. Another human iPS cell line, 201B7, generated from human dermal fibroblasts (HDF) was kindly provided by Dr. S. Yamanaka (Kyoto University) [6]. The human iPS cell line 201B7 was maintained on a feeder layer of mitomycin C-treated mouse embryonic fibroblasts with Repro Stem (Repro CELL), supplemented with 5 ng/ml FGF2 (Sigma). Human iPSCs were dissociated with 0.1 mg/ml dispase (Roche Diagnostics) into small clumps, and subcultured every 5 or 6 days.

Adenovirus (Ad) Vectors

Ad vectors were constructed by an improved *in vitro* ligation method [41,42]. The human SOX17 gene (accession number NM_022454) was amplified by PCR using primers designed to incorporate the 5′ BamHI and 3′ XbaI restriction enzyme sites: Fwd 5′-gcagggatccagcgccatgagcagcccgg-3′ and Rev 5′-cttctagagatcagggacctgtcacacgtc-3′. The human SOX17 gene was inserted into pcDNA3 (Invitrogen), resulting in pcDNA-SOX17, and then the human SOX17 gene was inserted into pHMEF5 [15], which contains the human EF-1α promoter, resulting in pHMEF-SOX17. The pHMEF-SOX17 was digested with I-CeuI/PI-SceI and ligated into I-CeuI/PI-SceI-digested pAdHM41-K7 [16], resulting in pAd-SOX17. The human elongation factor-1α (EF-1α) promoter-driven LacZ- or HEX-expressing Ad vectors, Ad-LacZ or Ad-HEX, were constructed previously. [13,43]. Ad-SOX17, Ad-HEX, and Ad-LacZ, which contain a stretch of lysine residue (K7) peptides in the C-terminal region of the fiber knob for more efficient transduction of human ESCs, iPSCs, and DE cells, were generated and purified as described previously [13,15,43]. The vector particle (VP) titer was determined by using a spectrophotometric method [44].

Flow Cytometry

Single-cell suspensions of human ESCs, iPSCs, and their derivatives were fixed with methanol at 4°C for 20 min, then incubated with the primary antibody, followed by the secondary antibody. Flow cytometry analysis was performed using a FACS LSR Fortessa flow cytometer (Becton Dickinson).

RNA Isolation and Reverse Transcription-Polymerase Chain Reaction (RT-PCR)

Total RNA was isolated from human ESCs, iPSCs, and their derivatives using ISOGENE (Nippon Gene) according to the manufacture's instructions. Primary human hepatocytes were purchased from CellzDirect. cDNA was synthesized using 500 ng of total RNA with a Superscript VILO cDNA synthesis kit (Invitrogen). Real-time RT-PCR was performed with Taqman gene expression assays (Applied Biosystems) or SYBR Premix Ex Taq (TaKaRa) using an ABI PRISM 7000 Sequence Detector (Applied Biosystems). Relative quantification was performed against a standard curve and the values were normalized against the input determined for the housekeeping gene, glyceraldehyde 3-phosphate dehydrogenase (GAPDH). The primer sequences used in this study are described in Table S1.

Immunohistochemistry

The cells were fixed with methanol or 4% PFA. After blocking with PBS containing 2% BSA and 0.2% Triton X-100 (Sigma), the cells were incubated with primary antibody at 4°C for 16 h, followed by incubation with a secondary antibody that was labeled

with Alexa Fluor 488 or Alexa Fluor 594 (Invitrogen) at room temperature for 1 h. All the antibodies are listed in Table S2.

Crystal Violet Staining

The human ESC-derived cells that had adhered to the wells were stained with 200 µl of 0.3% crystal violet solution at room temperature for 15 min. Excess crystal violet was then removed and the wells were washed three times. Fixed crystal violet was solubilized in 200 µl of 100% ethanol at room temperature for 15 min. Cell viability was estimated by measuring the absorbance at 595 nm of each well using a microtiter plate reader (Sunrise, Tecan).

LacZ Assay

The human ESC- and iPSC-derived cells were transduced with Ad-LacZ at 3,000 VP/cell for 1.5 h. After culturing for the indicated number of days, 5-bromo-4-chloro-3-indolyl β-D-galactopyranoside (X-Gal) staining was performed as described previously [15].

Supporting Information

Table S1 List of Taqman probes and primers used in this study.
(DOC)

Table S2 List of antibodies used in this study.
(DOC)

Figure S1 PrE cells formation from human ESCs on day 1 of differentiation. (A) The procedure for differentiation of human ESCs and iPSCs to ExEn cells by treatment with BMP4 (20 ng/ml) is presented schematically. (B) Human ESCs (H9) were morphologically changed during ExEn differentiation; when human ESCs were cultured with the medium containing BMP4 (20 ng/ml) for 5 days, the cells began to show flattened epithelial morphology. The scale bar represents 50 µm. (C–E) The tTemporal protein expression analysis during ExEn differentiation was performed by immunohistochemistry. The PrE markers COUP-TF1 [21] (red), SOX17 [14] (red), and SOX7 [14] (red) were detected on day 1. In contrast to the PS markers, the expression of the DE marker GSC [22] (red) was not detected and the level of the pluripotent marker NANOG (green) declined between day 0 and day 1. Nuclei were counterstained with DAPI (blue). The scale bar represents 50 µm.
(PDF)

Figure S2 Mesendoderm cells formation from human ESCs on day 3 of differentiation. (A) The procedure for differentiation of human ESCs and iPSCs to DE cells by treatment with Activin A (100 ng/ml) is presented schematically. hESF-GRO medium was supplemented with 5 factors and 0.5 mg/ml fatty acid free BSA, as described in the Materials and Methods. (B) Human ESCs (H9) were morphologically changed during DE differentiation; when human ESCs were cultured with the medium containing Activin A (100 ng/ml) for 5 days, the morphology of the cells began to show visible cell-cell boundaries. The scale bar represents 50 µm. (C–E) The tTemporal protein expression analysis during DE differentiation was performed by immunohistochemistry. The anterior PS markers FOXA2 [21] (red), GSC [22] (red), and SOX17 [14] (red) were adequately detected on day 3. The PS marker T [45] (red) was detected until day 3. In contrast to the PS markers, the expression of the pluripotent marker NANOG [24] (green) declined between day 2 and day 3. Nuclei were counterstained with DAPI (blue). The scale bar represents 50 µm.
(PDF)

Figure S3 Overexpression of SOX17 mRNA in human ESC (H9)-derived PS cells by Ad-SOX17 transduction. Human ESC-derived PS cells (day 1) were transduced with 3,000VP/cell of Ad-SOX17 for 1.5 h. On day 3 of differentiation, real-time RT-PCR analysis of the SOX17 expression was performed in Ad-LacZ-transduced cells and Ad-SOX17-transduced cells. On the y axis, the expression levels of undifferentiated human ESCs on day 0 was were taken defined as 1.0. All data are represented as the means±SD ($n = 3$).
(PDF)

Figure S4 Efficient transduction in Activin A-induced human ESC (H9)-derived cells by using a fiber-modified Ad vector containing the EF-1α promoter. Undifferentiated human ESCs and Activin A-induced human ESC-derived cells, which were cultured with the medium containing Activin A (100 ng/ml) for 0, 1, 2, 3, and 4 days, were transduced with 3,000 vector particles (VP)/cell of Ad-LacZ for 1.5 h. The day after transduction, X-gal staining was performed. The scale bar represents 100 µm. Similar results were obtained in two independent experiments.
(PDF)

Figure S5 Optimization of the time period for Ad-SOX17 transduction to promote DE differentiation from human iPSCs (Tic). Undifferentiated human iPSCs and Activin A-induced human iPSC-derived cells, which were cultured with the medium containing Activin A (100 ng/ml) for 0, 1, 2, 3, and 4 days, were transduced with 3,000 VP/cell of Ad-SOX17 for 1.5 h. Ad-SOX17-transduced cells were cultured with Activin A (100 ng/ml) until day 5, and then real-time RT-PCR analysis was performed. The horizontal axis represents the day on which the cells were transduced with Ad-SOX17. On the y axis, the expression levels of undifferentiated cells on day 0 was were taken defined as 1.0. All data are represented as the means±SD ($n = 3$).
(PDF)

Figure S6 Time course of LacZ expression in human ESC (H9)-derived mesendoderm cells transduced with Ad-LacZ. The hHuman ESC-derived mesendoderm cells (day 3) were transduced with 3,000 VP/cell of Ad-LacZ for 1.5 h. On days 4, 5, 6, 8, and 10, X-gal staining was performed. Note that human ESC-derived cells were passaged on day 5. The scale bar represents 100 µm. Similar results were obtained in two independent experiments.
(PDF)

Figure S7 Optimization of the time period for Ad-SOX17 transduction into Activin A-induced human ESC (H9)-derived cells. Undifferentiated human ESCs and Activin A-induced hESC-derived cells, which were cultured with the medium containing Activin A (100 ng/ml) for 0, 1, 2, 3, and 4 days, were transduced with 3,000 VP/cell of Ad-LacZ or Ad-SOX17 for 1.5 h. Ad-SOX17-transduced cells were cultured with Activin A (100 ng/ml) until day 5, then the cell viability was evaluated with crystal violet staining. The horizontal axis represents the day on which the cells were transduced with Ad-SOX17. On the y axis, the level of non-transduced cells was taken defined as 1.0. All data are represented as the means±SD (n = 3).
(PDF)

Figure S8 Model of differentiation of human ESCs and iPSCs into ExEn and DE cells by stage-specific SOX17 transduction. The ExEn and DE differentiation process is divided into at least two stages. In the first stage, human ESCs differentiate into either PrE cells by treatment with BMP4 (20 ng/ml) or mesendoderm cells by treatment with Activin A (100 ng/

ml). In the second stage, SOX17 promotes the further differentiation of each precursor cell into ExEn and DE cells, respectively. We have demonstrated that the efficient differentiation of these two distinct endoderm lineages is accomplished by stage-specific SOX17 transduction.
(PDF)

Acknowledgments

We thank Hiroko Matsumura and Misae Nishijima for their excellent technical support. We thank Mr. David Bennett and Ms. Ong Tyng Tyng for critical reading of the manuscript.

Author Contributions

Conceived and designed the experiments: K. Takayama MI K. Kawabata MFK HM. Performed the experiments: K. Takayama MI K. Tashiro. Analyzed the data: K. Takayama MI K. Kawabata K. Tashiro K. Katayama FS HM. Contributed reagents/materials/analysis tools: K. Kawabata K. Katayama FS TH MFK HM. Wrote the paper: K. Takayama K. Kawabata HM.

References

1. Enders AC, Given RL, Schlafke S (1978) Differentiation and migration of endoderm in the rat and mouse at implantation. Anat Rec 190: 65–77.
2. Gardner RL (1983) Origin and differentiation of extraembryonic tissues in the mouse. Int Rev Exp Pathol 24: 63–133.
3. Grapin-Botton A, Constam D (2007) Evolution of the mechanisms and molecular control of endoderm formation. Mech Dev 124: 253–278.
4. Tam PP, Kanai-Azuma M, Kanai Y (2003) Early endoderm development in vertebrates: lineage differentiation and morphogenetic function. Curr Opin Genet Dev 13: 393–400.
5. Thomson JA, Itskovitz-Eldor J, Shapiro SS, Waknitz MA, Swiergiel JJ, et al. (1998) Embryonic stem cell lines derived from human blastocysts. Science 282: 1145–1147.
6. Takahashi K, Tanabe K, Ohnuki M, Narita M, Ichisaka T, et al. (2007) Induction of pluripotent stem cells from adult human fibroblasts by defined factors. Cell 131: 861–872.
7. Yu J, Vodyanik MA, Smuga-Otto K, Antosiewicz-Bourget J, Frane JL, et al. (2007) Induced pluripotent stem cell lines derived from human somatic cells. Science 318: 1917–1920.
8. Xu RH, Chen X, Li DS, Li R, Addicks GC, et al. (2002) BMP4 initiates human embryonic stem cell differentiation to trophoblast. Nat Biotechnol 20: 1261–1264.
9. Pera MF, Andrade J, Houssami S, Reubinoff B, Trounson A, et al. (2004) Regulation of human embryonic stem cell differentiation by BMP-2 and its antagonist noggin. J Cell Sci 117: 1269–1280.
10. Seguin CA, Draper JS, Nagy A, Rossant J (2008) Establishment of endoderm progenitors by SOX transcription factor expression in human embryonic stem cells. Cell Stem Cell 3: 182–195.
11. Gouon-Evans V, Boussemart L, Gadue P, Nierhoff D, Koehler CI, et al. (2006) BMP-4 is required for hepatic specification of mouse embryonic stem cell-derived definitive endoderm. Nat Biotechnol 24: 1402–1411.
12. Niakan KK, Ji H, Maehr R, Vokes SA, Rodolfa KT, et al. (2010) Sox17 promotes differentiation in mouse embryonic stem cells by directly regulating extraembryonic gene expression and indirectly antagonizing self-renewal. Genes Dev 24: 312–326.
13. Inamura M, Kawabata K, Takayama K, Tashiro K, Sakurai F, et al. (2011) Efficient Generation of Hepatoblasts From Human ES Cells and iPS Cells by Transient Overexpression of Homeobox Gene HEX. Mol Ther 19: 400–407.
14. Kanai-Azuma M, Kanai Y, Gad JM, Tajima Y, Taya C, et al. (2002) Depletion of definitive gut endoderm in Sox17-null mutant mice. Development 129: 2367–2379.
15. Kawabata K, Sakurai F, Yamaguchi T, Hayakawa T, Mizuguchi H (2005) Efficient gene transfer into mouse embryonic stem cells with adenovirus vectors. Mol Ther 12: 547–554.
16. Koizumi N, Mizuguchi H, Utoguchi N, Watanabe Y, Hayakawa T (2003) Generation of fiber-modified adenovirus vectors containing heterologous peptides in both the HI loop and C terminus of the fiber knob. J Gene Med 5: 267–276.
17. Fujikura J, Yamato E, Yonemura S, Hosoda K, Masui S, et al. (2002) Differentiation of embryonic stem cells is induced by GATA factors. Genes Dev 16: 784–789.
18. Koutsourakis M, Langeveld A, Patient R, Beddington R, Grosveld F (1999) The transcription factor GATA6 is essential for early extraembryonic development. Development 126: 723–732.
19. Morrisey EE, Tang Z, Sigrist K, Lu MM, Jiang F, et al. (1998) GATA6 regulates HNF4 and is required for differentiation of visceral endoderm in the mouse embryo. Genes Dev 12: 3579–3590.
20. Kunath T, Strumpf D, Rossant J (2004) Early trophoblast determination and stem cell maintenance in the mouse—a review. Placenta 25 Suppl A: S32–38.
21. Sasaki H, Hogan BL (1993) Differential expression of multiple fork head related genes during gastrulation and axial pattern formation in the mouse embryo. Development 118: 47–59.
22. Blum M, Gaunt SJ, Cho KW, Steinbeisser H, Blumberg B, et al. (1992) Gastrulation in the mouse: the role of the homeobox gene goosecoid. Cell 69: 1097–1106.
23. Morrison GM, Oikonomopoulou I, Migueles RP, Soneji S, Livigni A, et al. (2008) Anterior definitive endoderm from ESCs reveals a role for FGF signaling. Cell Stem Cell 3: 402–415.
24. Mitsui K, Tokuzawa Y, Itoh H, Segawa K, Murakami M, et al. (2003) The homeoprotein Nanog is required for maintenance of pluripotency in mouse epiblast and ES cells. Cell 113: 631–642.
25. Shalaby F, Rossant J, Yamaguchi TP, Gertsenstein M, Wu XF, et al. (1995) Failure of blood-island formation and vasculogenesis in Flk-1-deficient mice. Nature 376: 62–66.
26. D'Amour KA, Agulnick AD, Eliazer S, Kelly OG, Kroon E, et al. (2005) Efficient differentiation of human embryonic stem cells to definitive endoderm. Nat Biotechnol 23: 1534–1541.
27. Shiojiri N (1984) The origin of intrahepatic bile duct cells in the mouse. J Embryol Exp Morphol 79: 25–39.
28. Ingelman-Sundberg M, Oscarson M, McLellan RA (1999) Polymorphic human cytochrome P450 enzymes: an opportunity for individualized drug treatment. Trends Pharmacol Sci 20: 342–349.
29. Murry CE, Keller G (2008) Differentiation of embryonic stem cells to clinically relevant populations: lessons from embryonic development. Cell 132: 661–680.
30. Qu XB, Pan J, Zhang C, Huang SY (2008) Sox17 facilitates the differentiation of mouse embryonic stem cells into primitive and definitive endoderm in vitro. Dev Growth Differ 50: 585–593.
31. Sherwood RI, Jitianu C, Cleaver O, Shaywitz DA, Lamenzo JO, et al. (2007) Prospective isolation and global gene expression analysis of definitive and visceral endoderm. Dev Biol 304: 541–555.
32. Shimoda M, Kanai-Azuma M, Hara K, Miyazaki S, Kanai Y, et al. (2007) Sox17 plays a substantial role in late-stage differentiation of the extraembryonic endoderm in vitro. J Cell Sci 120: 3859–3869.
33. Yasunaga M, Tada S, Torikai-Nishikawa S, Nakano Y, Okada M, et al. (2005) Induction and monitoring of definitive and visceral endoderm differentiation of mouse ES cells. Nat Biotechnol 23: 1542–1550.
34. Gadue P, Huber TL, Paddison PJ, Keller GM (2006) Wnt and TGF-beta signaling are required for the induction of an in vitro model of primitive streak formation using embryonic stem cells. Proc Natl Acad Sci U S A 103: 16806–16811.
35. Levinson-Dushnik M, Benvenisty N (1997) Involvement of hepatocyte nuclear factor 3 in endoderm differentiation of embryonic stem cells. Mol Cell Biol 17: 3817–3822.
36. Spence JR, Lange AW, Lin SC, Kaestner KH, Lowy AM, et al. (2009) Sox17 regulates organ lineage segregation of ventral foregut progenitor cells. Dev Cell 17: 62–74.
37. Mizuguchi H, Hayakawa T (2004) Targeted adenovirus vectors. Hum Gene Ther 15: 1034–1044.
38. Furue MK, Na J, Jackson JP, Okamoto T, Jones M, et al. (2008) Heparin promotes the growth of human embryonic stem cells in a defined serum-free medium. Proc Natl Acad Sci U S A 105: 13409–13414.
39. Makino H, Toyoda M, Matsumoto K, Saito H, Nishino K, et al. (2009) Mesenchymal to embryonic incomplete transition of human cells by chimeric OCT4/3 (POU5F1) with physiological co-activator EWS. Exp Cell Res 315: 2727–2740.
40. Nagata S, Toyoda M, Yamaguchi S, Hirano K, Makino H, et al. (2009) Efficient reprogramming of human and mouse primary extra-embryonic cells to pluripotent stem cells. Genes Cells 14: 1395–1404.
41. Mizuguchi H, Kay MA (1998) Efficient construction of a recombinant adenovirus vector by an improved in vitro ligation method. Hum Gene Ther 9: 2577–2583.
42. Mizuguchi H, Kay MA (1999) A simple method for constructing E1- and E1/E4-deleted recombinant adenoviral vectors. Hum Gene Ther 10: 2013–2017.
43. Tashiro K, Kawabata K, Sakurai H, Kurachi S, Sakurai F, et al. (2008) Efficient adenovirus vector-mediated PPAR gamma gene transfer into mouse embryoid bodies promotes adipocyte differentiation. J Gene Med 10: 498–507.
44. Maizel JV, Jr., White DO, Scharff MD (1968) The polypeptides of adenovirus. I. Evidence for multiple protein components in the virion and a comparison of types 2, 7A, and 12. Virology 36: 115–125.
45. Wilkinson DG, Bhatt S, Herrmann BG (1990) Expression pattern of the mouse T gene and its role in mesoderm formation. Nature 343: 657–659.

J Artif Organs (2011) 14:171–177
DOI 10.1007/s10047-011-0578-4

MINIREVIEW

Tissue engineering and cell-based therapy toward integrated strategy with artificial organs

Satoshi Gojo · Masashi Toyoda · Akihiro Umezawa

Received: 9 May 2011 / Accepted: 19 May 2011 / Published online: 10 June 2011

Abstract Research in order that artificial organs can supplement or completely replace the functions of impaired or damaged tissues and internal organs has been underway for many years. The recent clinical development of implantable left ventricular assist devices has revolutionized the treatment of patients with heart failure. The emerging field of regenerative medicine, which uses human cells and tissues to regenerate internal organs, is now advancing from basic and clinical research to clinical application. In this review, we focus on the novel biomaterials, i.e., fusion protein, and approaches such as three-dimensional and whole-organ tissue engineering. We also compare induced pluripotent stem cells, directly reprogrammed cardiomyocytes, and somatic stem cells for cell source of future cell-based therapy. Integrated strategy of artificial organ and tissue engineering/regenerative medicine should give rise to a new era of medical treatment to organ failure.

This article is a translation of an article that appeared in *The Japanese Journal of Artificial Organs* 2010;39:202–207.

S. Gojo (✉)
Department of Therapeutic Strategy for Heart Failure,
Graduate School of Medicine, University of Tokyo,
7-3-1 Hongo, Bunkyo, Tokyo 113-8655, Japan
e-mail: satoshigojo-tky@umin.ac.jp

M. Toyoda
Research Team for Vascular Medicine,
Tokyo Metropolitan Institute of Gerontology, Tokyo, Japan

A. Umezawa (✉)
Department of Reproductive Biology,
National Institute for Child Health and Development,
2-10-1, Okura, Setagaya, Tokyo 157-8535, Japan
e-mail: umezawa@1985.jukuin.keio.ac.jp

Keywords Biofabrication · Stem cell · Reprogramming · Direct conversion · Clinical trial

Introduction

The human body is made up of approximately 60 trillion cells but can be traced back to one fertilized egg created by the union of an ovum and a sperm. The fertilized egg divides repeatedly, creating various cells that coordinate with each other to form all the different tissues and organs, ultimately leading to the formation of a complete individual. Whereas the human genome has been almost completely decoded and the genes involved in various mechanisms of the body are becoming known, many parts of this epic developmental process remain unclear. However, because these developmental mechanisms are closely related to the homeostatic maintenance and the regenerative mechanisms of organs and tissues, the field of regenerative medicine, which aims to use these mechanisms to treat diseases, is expanding rapidly.

Tissue engineering

Fusion protein

Biological tissue is composed not only of cells but also of a surrounding environment that is crucial in maintaining cell function in vivo and in homeostasis. Most importantly, the extracellular matrix is known to have dynamic and functional roles, such as providing a scaffold for cell adhesion (basement membrane and fibronectins) as well as maintaining and providing growth factors (heparan sulfate). Technological development with respect to manipulating

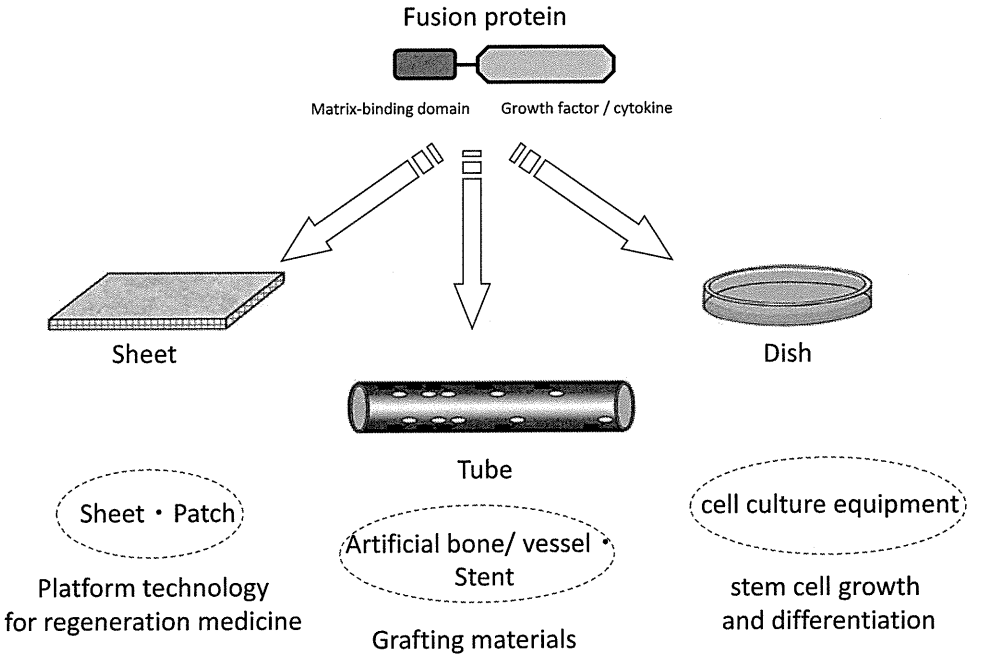

Fig. 1 Tissue engineering for regenerative medicine

this extracellular matrix in order to control tissues and cells, and its subsequent application in regenerative medicine, is underway. For example, studies have revealed that a variety of growth factors play important roles in wound healing, and some of these growth factors are in clinical use. However, the short-term effects of these growth factors pose some limitations on their use. An example is provided by fibrin, which is released in the wounded area when tissue damage occurs. An increasing amount of research is being conducted on the use of fibrin as a material for tissue regeneration. If a protein produced by the fusion of a fibrin-binding domain (FBD) to epidermal growth factor (EGF) is added to an epidermal wound-model culture system, binding of the growth factor to the fibrin released from the wound leads to healing by stimulating growth in the surrounding cells [1]. This phenomenon presumably occurs not because of the independent function of the growth factor, but because the growth factor stabilizes after binding to fibrin, and the FBD–EGF complex causes continuous cell stimulation. This suggests that the process of altering the combination of extracellular matrix and growth factors can be of therapeutic value in a variety of conditions. Another example can be considered with respect to vascular grafts. The development of small-caliber vascular grafts, such as those used to treat coronary artery disease, has slowed down because these grafts tend to fail at an early stage owing to thrombotic occlusion. To prevent this, prompt graft endothelialization and prevention of blood clot adherence is necessary. The use of a protein produced by fusion of the collagen-binding domain (CBD)—which binds collagen (a component of the extracellular matrix)—to hepatocyte growth factor (HGF) has been considered in such cases, and it has been shown that this complex (CBD–HGF) effectively promotes growth of endothelial cells [2]. Furthermore, this type of fusion protein could be placed onto a biodegradable sheet of extracellular matrix and affixed to the wounded area, where it may stimulate vascular cell growth. This has the potential for a wide application in medicine (Fig. 1).

Three-dimensional tissue engineering

A substantial amount of tissue engineering research has been performed on the three-piece that are cell, growth factors, and scaffolds. There are, however, various limitations to using scaffolds. First, cells tend to be distributed over the surface of the scaffold, thus making it difficult to form a solid tissue. Second, a 3D array and structure cannot be controlled when multiple cell types are used. Third, the concentration gradient of growth factors cannot be controlled. Fourth, there are certain limitations to the process of creating the vasa vasorum by tissue engineering techniques. In recent years, the concept of the scaffold has been put aside, and attempts to construct 3D tissue with cells and growth factors are now frequently reported. This method is generally called biofabrication [3], and the techniques of bioprinting [4] and organ printing [5] also fit into this category. In addition, although 3D structures using inkjet printer technology have already appeared as rapid prototyping, a 3D printer with an inkjet nozzle from which

droplets with a volume identical to that of cells are embossed, and which can be operated in a sterile environment, has been developed [6]. This could make the construction of 3D tissues possible [7]. Biorapid prototyping, a method in which many cellular spheres are used together with arbitrary structures to create 3D tissue, has also been reported [8]. This is expected to be an extremely promising methodology despite many issues, such as those related to cell solvents.

Cell sheets

Of all the recently developed tissue engineering techniques, practical application of cell sheets has advanced the most. This technology is based on the properties of a temperature-responsive polymer, poly(*N*-isopropylacrylamide). Culture dishes coated with this material are hydrophobic at 37°C and hydrophilic <32°C. When cells are cultured to confluence, they can be recovered as a sheet without enzymatic digestion [9]. This technique has been made available from Japan for worldwide application in the development of regenerative medicine-related products [10]. It was reported that stratification, which was initially limited to a few layers, could evolve to include many layers with neovascularization. So far, cell sheets have been made that consist of myoblasts [11], mesenchymal stem cells [12], cardiac progenitor cells [13], and a mixture of fibroblasts and endothelial progenitors [14]. Osaka University is coordinating a clinical trial using autologous myoblast sheets in patients carrying a left ventricular assist device (LVAD) with the aim of providing a bridge to recovery. In France, a clinical trial using epithelial cell sheets for corneal regeneration is being conducted by a venture company.

Whole-organ tissue engineering

The technology of perfusion decellularization of organs is a unique method of tissue production using scaffolds that has been reported in recent years. Intracellular structures can be completely eliminated by perfusing the heart using a Langendorff coronary perfusion apparatus for more than 12 h with the surfactant sodium dodecyl sulfate. It has also been reported that components of the extracellular matrix, including collagen type I/III, laminin, and fibronectin, can be preserved without disturbing their array structure; furthermore, the structure of valves and basal membrane of the epicardial vessels are not affected [15]. A heartbeat, albeit faint, has been achieved using this technique. The feasibility of whole-organ decellularization has been demonstrated in the pig heart [16] and rat liver [17]. Although the process of cellularization has its flaws, it is a creative initiative that holds promise for future developments.

Regenerative medicine

Induced pluripotent stem cells (iPSC)

The term regenerative medicine was introduced in 2000. Clinical applications have increased greatly since then, beginning with research on human embryonic stem cells (ESC) and confirmation of the plasticity of somatic stem cells. Amid frustration that human ESC could not be applicable not only to medicine, but also in biological research, the phenomenon of initialization via nuclear transplantation has been achieved in an elaborately planned experiment with four gene transfers. Now, these cells, called induced pluripotent stem cells (iPSC), certainly appear to be a major topic in regenerative medicine. Basic research into the clinical application of iPSC demonstrated the successful treatment of model mice for Parkinson's disease [18], sickle cell anemia [19], and hemophilia [20] with mouse iPSC. These reports indicate the same scheme could be applicable to human diseases. However, problems in iPSC application include the development of teratomas from undifferentiated cells, carcinomas due to gene transfer, and infection with xenogeneic materials used in cell cultures. These problems have attracted the interest of a large number of researchers, and many proposals for solutions to them have been reported (Fig. 2).

Teratoma formation in mice can reportedly be prevented by eliminating stage-specific embryonic antigen-1-positive cells [18]. If the target of interest is the heart, enrichment with mitochondria could prevent teratoma formation [21]. Of the four genes transferred during iPSC initialization, which are considered to be reprogramming genes, it was feared that the existence of c-Myc, in particular, which is an oncogene, would lead to cancer; carcinogenesis through c-Myc reactivation was actually observed in vivo. In addition, because the basic protocol uses a retrovirus as the vector for gene transfer, the possibility of carcinogenesis after its insertion into a genome is a problem. It was subsequently reported that just three factors (excluding c-Myc) induced iPSC, albeit at a low frequency [22]. However, recently, induction of iPSC with RNA [23] and proteins [24] of reprogramming factors has been reported in an attempt to circumvent carcinogenesis because of the methodology. Of the four factors, Sox2 and c-Myc could be replaced with transforming growth factor-α receptor antagonists [25], the nuclear acceptor Esrrb could be replaced with Klf4 [26], and Oct4 could be replaced with nuclear acceptor Nr5a2 [27].

Currently, xenogeneic materials are used in various processes in standard ESC/iPSC culture (Fig. 3). Feeder cells are used to maintain the undifferentiated state of both ESC and iPSC; usually, mouse embryonic fibroblasts (MEF) treated with mitomycin C to arrest their growth are

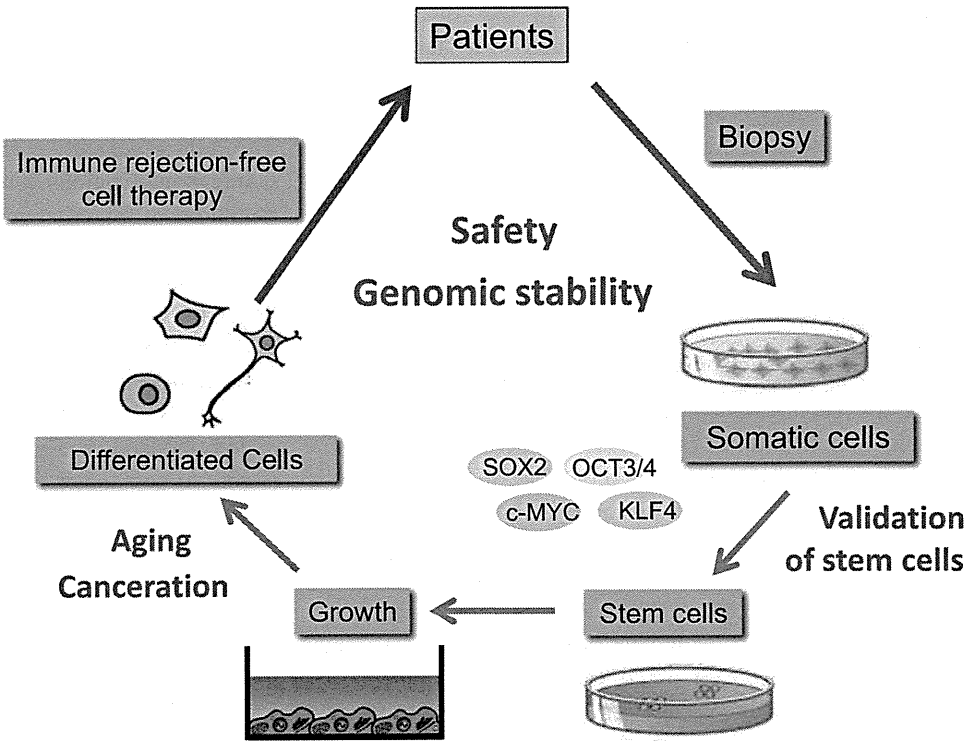

Fig. 2 Order-made stem cell therapy

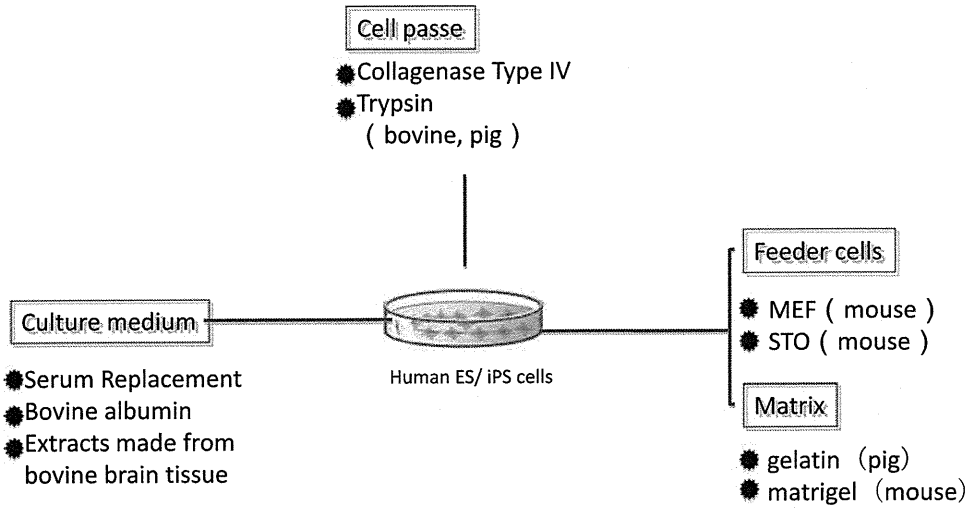

Fig. 3 Xenogeneic factors and materials in human embryonic stem cell/induced pluripotent stem cell (ESC/iPSC) culture

used as feeder cells. It was feared that if these xenogeneic cells were used in clinical situations, contamination with xenogeneic cells may lead to infection. This did, in fact, occur: the presence of non-human-derived Neu5Gc was confirmed on the cell surface of human ESC cultured onto MEF. Many individuals possess antibodies for this antigen, and an immune reaction can be provoked in these individuals [28]. In order to avoid xenogeneic contamination, coating cell culture dishes with fully synthetic compounds and the chemical defined-culture medium has been reported from several institutes. A 3D porous natural polymer scaffold consisting of chitosan and alginate was able to sustain human ESC self-renewal [29]. Recombinant vitronectin also supported cultivation of three human ESC under feeder-free conditions [30]. Moreover, suspension culture of human ESC and iPSC in chemically defined media supplied a scalable number of cells [31]. However, the ability of xeno-free protocols to maintain the self-renewal ability and pluripotency of human ESC or iPSC remains questionable. On the other hand, autologous

fibroblasts could be used as feeder cells in the culture of human iPSC [32].

Almost the entire process of reprogramming in iPSC remains poorly understood. It is still unclear whether iPSC reprogramming is equal to nuclear transplantation, which showed that the somatic nucleus reacquired totipotency. The following factors imply that multiple processes exist in reprogramming: the expression of stem cell-related genes differs between iPSC clones [33], and "memories" of the parent cells remain. It has been reported that trichostatin A, a histone deacetylase inhibitor, is a factor that promotes this phenomenon [34]. The necessity of using it under strictly controlled temporal and quantitative requirements indicates the preciseness of its mechanism.

Direct conversion to differentiated cells

The phenomenon termed direct conversion to differentiated cells is a novel occurrence recently reported to occur in several organs. Although many researchers have searched for the master gene, such as MyoD, that can induce formation of skeletal muscle cells from fibroblasts, no such gene has been discovered. However, because the use of four genes allows the differentiated cell to have pluripotency, transformation with one batch of gene transfer is been investigated. A first report described successful differentiation of pancreatic exocrine cells into insulin-secreting beta-like cells by the transfer of three genes (Ngn3/Pdx1/MafA) [35]. Another report documented successful induction of cells expressing myocardial cell structural proteins through the transfer of Gata4/Tbx5/Baf60c into mouse mesodermal cells [36]. According to later reports, functional neurons can be induced by transferring Asc11/Brn2/Myt11 into fibroblasts [37], and myocardial cells can be induced by transferring Gata4/Tbx5/Mef2c into fibroblasts [38]. Thus far, the possibility that these cells only caused specific gene expression that exists in the lower area of transgenes cannot be denied. Functional and quantitative assessments of induced cells produced by direct reprogramming are required to determine their application in the clinical setting.

Somatic stem cells

It was long believed that cardiomyocytes were in a state of terminal differentiation in adults and that the heart cannot heal itself or restore its homeostatic functions. These properties led researchers in cardiac regeneration to increased interest in somatic stem cells, including bone-marrow-derived stem/progenitor cells, mesenchymal stem cells, and adipose-derived stem cells. Because cells derived from fetal-related tissue (including the amnion, umbilical cord, and placenta) contain a multipotent population that shows plasticity, many organizations, institutes, and companies run banking systems for these cells. Transplantation of amniocytes caused cardiac regeneration in myocardial infarction in rats [39]. On the other hand, other researchers have continually asserted the heart has regenerative properties. Recently, clear evidence that cardiomyocytes can be reborn in the adult heart was reported. This evidence was based on cardiomyocyte age estimation by measuring carbon-14, which was generated by nuclear weapons testing during the Cold War [40]. The impetus for the expansion of this field of study was the reporting of a method that was apparently based on embryonic bodies [41]: by forming a sphere with cardiac-tissue-derived cells, a group of nearly undifferentiated cells could be enriched. Subsequently, several groups reported that stem cells and precursor cells exist in the heart. Several profiles were reported for these cells, including c-kit (+) [42], sca-1 (+) [43], and side population cells [44]. Whether this means that we are observing the process of differentiation as it develops or that multiple stem cell systems exist is an issue that needs to be addressed. Matsubara et al. [45], who reported that murine sca-1 (+) cells could be cardiac stem cells (CSC), performed a detailed preclinical study in pigs to treat ischemic heart disease [46] and are directing the world's first clinical trial using CSC. This clinical trial targets patients with severe chronic ischemic heart failure whose left ventricular ejection fraction is <35%. The method involves intramuscular injection of CSC during coronary artery bypass grafting. The injected stem cells are isolated from cardiac tissue collected during a previous biopsy from the right ventricular septal region. During cell culture, recombinant basic fibroblast growth factor (bFGF) is used rather than xenogeneic materials, and blood serum is obtained from autologous blood. The cells are injected through the epicardium, and the injection sites are covered with a basic sustained-release gelatin sheet of bFGF. Patients are not randomized, and six cases are scheduled for an open-label phase I/IIa clinical trial, with a planned 1-year follow-up study. It is assumed that after this trial, cases will accumulate in multifacility clinical studies and that this method will develop into a highly advanced medical technology.

Chemical pharmacology is faced with difficulty finding new classes of drugs despite increasing budgets. Cells and tissues, therefore, are likely to become important medical treatments. Moreover, integrated therapy of ventricular assist device (VAD) and regenerative medicine should have great potential to treat severe heart failure (Fig. 4). Although implantable VADs are being used with excellent prognosis, many issues remain; for example, right ventricular failure, infection, thrombosis, and device mechanical failure. A market report on VAD anticipates that the "bridge to recovery (BTR)" strategy will constitute more

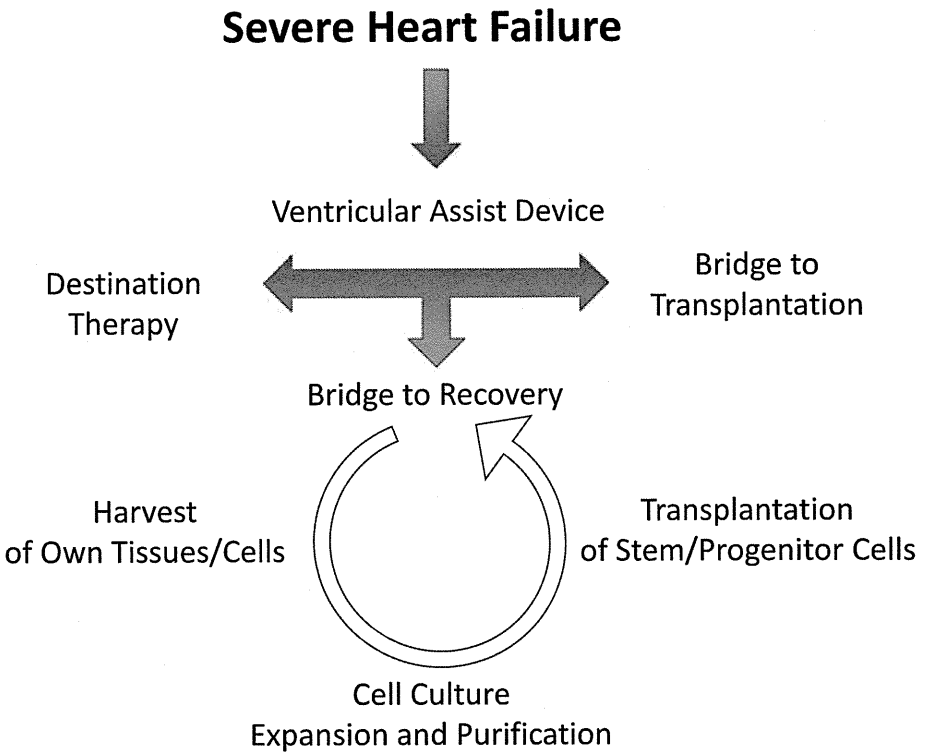

Fig. 4 Integrated strategy to heart failure

than half of future VAD therapy. The emerging field of regenerative medicine will surely accelerate the trend to BTR therapy.

References

1. Kitajima T, Sakuragi M, Hasuda H, Ozu T, Ito Y. A chimeric epidermal growth factor with fibrin affinity promotes repair of injured keratinocyte sheets. Acta Biomater. 2009;5:2623–32.
2. Ohkawara N, Ueda H, Shinozaki S, Kitajima T, Ito Y, Asaoka H, Kawakami A, Kaneko E, Shimokado K. Hepatocyte growth factor fusion protein having collagen-binding activity (CBD-HGF) accelerates re-endothelialization and intimal hyperplasia in balloon-injured rat carotid artery. J Atheroscler Thromb. 2007;14:185–91.
3. Mironov V, Trusk T, Kasyanov V, Little S, Swaja R, Markwald R. Biofabrication: a 21st century manufacturing paradigm. Biofabrication. 2009;1:022001.
4. Jakab K, Norotte C, Marga F, Murphy K, Vunjak-Novakovic G, Forgacs G. Tissue engineering by self-assembly and bio-printing of living cells. Biofabrication. 2010;2:022001.
5. Visconti RP, Kasyanov V, Gentile C, Zhang J, Markwald RR, Mironov V. Towards organ printing: engineering an intra-organ branched vascular tree. Expert Opin Biol Ther. 2010;10:409–20.
6. Nishiyama Y, Nakamura M, Henmi C, Yamaguchi K, Mochizuki S, Nakagawa H, Takiura K. Development of a three-dimensional bioprinter: construction of cell supporting structures using hydrogel and state-of-the-art inkjet technology. J Biomech Eng. 2009;131:035001.
7. Norotte C, Marga FS, Niklason LE, Forgacs G. Scaffold-free vascular tissue engineering using bioprinting. Biomaterials. 2009;30:5910–7.
8. Iwami K, Noda T, Ishida K, Morishima K, Nakamura M, Umeda N. Bio rapid prototyping by extruding/aspirating/refilling thermoreversible hydrogel. Biofabrication. 2010;2:014108.
9. Shimizu T, Yamato M, Kikuchi A, Okano T. Two-dimensional manipulation of cardiac myocyte sheets utilizing temperature-responsive culture dishes augments the pulsatile amplitude. Tissue Eng. 2001;7:141–51.
10. Shimizu T, Sekine H, Yamato M, Okano T. Cell sheet-based myocardial tissue engineering: new hope for damaged heart rescue. Curr Pharm Des. 2009;15:2807–14.
11. Miyagawa S, Saito A, Sakaguchi T, Yoshikawa Y, Yamauchi T, Imanishi Y, Kawaguchi N, Teramoto N, Matsuura N, Iida H, Shimizu T, Okano T, Sawa Y. Impaired myocardium regeneration with skeletal cell sheets—a preclinical trial for tissue-engineered regeneration therapy. Transplantation. 2010;90:364–72.
12. Hida N, Nishiyama N, Miyoshi S, Kira S, Segawa K, Uyama T, Mori T, Miyado K, Ikegami Y, Cui C, Kiyono T, Kyo S, Shimizu T, Okano T, Sakamoto M, Ogawa S, Umezawa A. Novel cardiac precursor-like cells from human menstrual blood-derived mesenchymal cells. Stem Cells. 2008;26:1695–704.
13. Fedak PW. Cardiac progenitor cell sheet regenerates myocardium and renews hope for translation. Cardiovasc Res. 2010;87:8–9.
14. Kobayashi H, Shimizu T, Yamato M, Tono K, Masuda H, Asahara T, Kasanuki H, Okano T. Fibroblast sheets co-cultured with endothelial progenitor cells improve cardiac function of infarcted hearts. J Artif Organs. 2008;11:141–7.
15. Ott HC, Matthiesen TS, Goh SK, Black LD, Kren SM, Netoff TI, Taylor DA. Perfusion-decellularized matrix: using nature's platform to engineer a bioartificial heart. Nat Med. 2008;14:213–21.
16. Wainwright JM, Czajka CA, Patel UB, Freytes DO, Tobita K, Gilbert TW, Badylak SF. Preparation of cardiac extracellular matrix from an intact porcine heart. Tissue Eng Part C Methods. 2010;16:525–32.
17. Soto-Gutierrez A, Zhang L, Medberry C, Fukumitsu K, Faulk D, Jiang H, Reing J, Gramignoli R, Komori J, Ross M, Nagaya M, Lagasse E, Stolz D, Strom SC, Fox IJ, Badylak SF.

A Whole-organ regenerative medicine approach for liver replacement. Tissue Eng Part C Methods 2011.
18. Wernig M, Zhao JP, Pruszak J, Hedlund E, Fu D, Soldner F, Broccoli V, Constantine-Paton M, Isacson O, Jaenisch R. Neurons derived from reprogrammed fibroblasts functionally integrate into the fetal brain and improve symptoms of rats with Parkinson's disease. Proc Natl Acad Sci USA. 2008;105:5856–61.
19. Hanna J, Wernig M, Markoulaki S, Sun CW, Meissner A, Cassady JP, Beard C, Brambrink T, Wu LC, Townes TM, Jaenisch R. Treatment of sickle cell anemia mouse model with iPS cells generated from autologous skin. Science. 2007;318:1920–3.
20. Xu D, Alipio Z, Fink LM, Adcock DM, Yang J, Ward DC, Ma Y. Phenotypic correction of murine hemophilia A using an iPS cell-based therapy. Proc Natl Acad Sci USA. 2009;106:808–13.
21. Hattori F, Chen H, Yamashita H, Tohyama S, Satoh YS, Yuasa S, Li W, Yamakawa H, Tanaka T, Onitsuka T, Shimoji K, Ohno Y, Egashira T, Kaneda R, Murata M, Hidaka K, Morisaki T, Sasaki E, Suzuki T, Sano M, Makino S, Oikawa S, Fukuda K. Nongenetic method for purifying stem cell-derived cardiomyocytes. Nat Methods. 2010;7:61–6.
22. Nakagawa M, Koyanagi M, Tanabe K, Takahashi K, Ichisaka T, Aoi T, Okita K, Mochiduki Y, Takizawa N, Yamanaka S. Generation of induced pluripotent stem cells without Myc from mouse and human fibroblasts. Nat Biotechnol. 2008;26:101–6.
23. Warren L, Manos PD, Ahfeldt T, Loh YH, Li H, Lau F, Ebina W, Mandal PK, Smith ZD, Meissner A, Daley GQ, Brack AS, Collins JJ, Cowan C, Schlaeger TM, Rossi DJ. Highly efficient reprogramming to pluripotency and directed differentiation of human cells with synthetic modified mRNA. Cell Stem Cell. 2010;7:618–30.
24. Kim D, Kim CH, Moon JI, Chung YG, Chang MY, Han BS, Ko S, Yang E, Cha KY, Lanza R, Kim KS. Generation of human induced pluripotent stem cells by direct delivery of reprogramming proteins. Cell Stem Cell. 2009;4:472–6.
25. Maherali N, Hochedlinger K. Tgfbeta signal inhibition cooperates in the induction of iPSCs and replaces Sox2 and cMyc. Curr Biol. 2009;19:1718–23.
26. Feng B, Jiang J, Kraus P, Ng JH, Heng JC, Chan YS, Yaw LP, Zhang W, Loh YH, Han J, Vega VB, Cacheux-Rataboul V, Lim B, Lufkin T, Ng HH. Reprogramming of fibroblasts into induced pluripotent stem cells with orphan nuclear receptor Esrrb. Nat Cell Biol. 2009;11:197–203.
27. Heng JC, Feng B, Han J, Jiang J, Kraus P, Ng JH, Orlov YL, Huss M, Yang L, Lufkin T, Lim B, Ng HH. The nuclear receptor Nr5a2 can replace Oct4 in the reprogramming of murine somatic cells to pluripotent cells. Cell Stem Cell. 2010;6:167–74.
28. Martin MJ, Muotri A, Gage F, Varki A. Human embryonic stem cells express an immunogenic nonhuman sialic acid. Nat Med. 2005;11:228–32.
29. Li Z, Leung M, Hopper R, Ellenbogen R, Zhang M. Feeder-free self-renewal of human embryonic stem cells in 3D porous natural polymer scaffolds. Biomaterials. 2010;31:404–12.
30. Braam SR, Zeinstra L, Litjens S, Ward-van Oostwaard D, van den BS, van Laake L, Lebrin F, Kats P, Hochstenbach R, Passier R, Sonnenberg A, Mummery CL, et al. Recombinant vitronectin is a functionally defined substrate that supports human embryonic stem cell self-renewal via alphavbeta5 integrin. Stem Cells. 2008;26:2257–65.
31. Olmer R, Haase A, Merkert S, Cui W, Palecek J, Ran C, Kirschning A, Scheper T, Glage S, Miller K, Curnow EC, Hayes ES, Martin U. Long term expansion of undifferentiated human iPS and ES cells in suspension culture using a defined medium. Stem Cell Res. 2010;5:51–64.
32. Takahashi K, Narita M, Yokura M, Ichisaka T, Yamanaka S. Human induced pluripotent stem cells on autologous feeders. PLoS One. 2009;4:e8067.
33. Miura K, Okada Y, Aoi T, Okada A, Takahashi K, Okita K, Nakagawa M, Koyanagi M, Tanabe K, Ohnuki M, Ogawa D, Ikeda E, Okano H, Yamanaka S. Variation in the safety of induced pluripotent stem cell lines. Nat Biotechnol. 2009;27:743–5.
34. Kishigami S, Van Thuan N, Hikichi T, Ohta H, Wakayama S, Mizutani E, Wakayama T. Epigenetic abnormalities of the mouse paternal zygotic genome associated with microinsemination of round spermatids. Dev Biol. 2006;289:195–205.
35. Zhou Q, Brown J, Kanarek A, Rajagopal J, Melton DA. In vivo reprogramming of adult pancreatic exocrine cells to beta-cells. Nature. 2008;455:627–32.
36. Takeuchi JK, Bruneau BG. Directed transdifferentiation of mouse mesoderm to heart tissue by defined factors. Nature. 2009;459:708–11.
37. Vierbuchen T, Ostermeier A, Pang ZP, Kokubu Y, Sudhof TC, Wernig M. Direct conversion of fibroblasts to functional neurons by defined factors. Nature. 2010;463:1035–41.
38. Ieda M, Fu JD, Delgado-Olguin P, Vedantham V, Hayashi Y, Bruneau BG, Srivastava D. Direct reprogramming of fibroblasts into functional cardiomyocytes by defined factors. Cell. 2010;142:375–86.
39. Tsuji H, Miyoshi S, Ikegami Y, Hida N, Asada H, Togashi I, Suzuki J, Satake M, Nakamizo H, Tanaka M, Mori T, Segawa K, Nishiyama N, Inoue J, Makino H, Miyado K, Ogawa S, Yoshimura Y, Umezawa A. Xenografted human amniotic membrane-derived mesenchymal stem cells are immunologically tolerated and transdifferentiated into cardiomyocytes. Circ Res. 2010;106:1613–23.
40. Bergmann O, Bhardwaj RD, Bernard S, Zdunek S, Barnabe-Heider F, Walsh S, Zupicich J, Alkass K, Buchholz BA, Druid H, Jovinge S, Frisen J. Evidence for cardiomyocyte renewal in humanso. Science. 2009;324:98–102.
41. Messina E, De Angelis L, Frati G, Morrone S, Chimenti S, Fiordaliso F, Salio M, Battaglia M, Latronico MV, Coletta M, Vivarelli E, Frati L, Cossu G, Giacomello A. Isolation and expansion of adult cardiac stem cells from human and murine heart. Circ Res. 2004;95:911–21.
42. Beltrami AP, Barlucchi L, Torella D, Baker M, Limana F, Chimenti S, Kasahara H, Rota M, Musso E, Urbanek K, Leri A, Kajstura J, Nadal-Ginard B, Anversa P. Adult cardiac stem cells are multipotent and support myocardial regeneration. Cell. 2003;114:763–76.
43. Matsuura K, Nagai T, Nishigaki N, Oyama T, Nishi J, Wada H, Sano M, Toko H, Akazawa H, Sato T, Nakaya H, Kasanuki H, Komuro I. Adult cardiac Sca-1-positive cells differentiate into beating cardiomyocytes. J Biol Chem. 2004;279:11384–91.
44. Martin CM, Meeson AP, Robertson SM, Hawke TJ, Richardson JA, Bates S, Goetsch SC, Gallardo TD, Garry DJ. Persistent expression of the ATP-binding cassette transporter, Abcg2, identifies cardiac SP cells in the developing and adult heart. Dev Biol. 2004;265:262–75.
45. Tateishi K, Ashihara E, Takehara N, Nomura T, Honsho S, Nakagami T, Morikawa S, Takahashi T, Ueyama T, Matsubara H, Oh H. Clonally amplified cardiac stem cells are regulated by Sca-1 signaling for efficient cardiovascular regeneration. J Cell Sci. 2007;120:1791–800.
46. Takehara N, Tsutsumi Y, Tateishi K, Ogata T, Tanaka H, Ueyama T, Takahashi T, Takamatsu T, Fukushima M, Komeda M, Yamagishi M, Yaku H, Tabata Y, Matsubara H, Oh H. Controlled delivery of basic fibroblast growth factor promotes human cardiosphere-derived cell engraftment to enhance cardiac repair for chronic myocardial infarction. J Am Coll Cardiol. 2008;52:1858–65.

J Artif Organs (2011) 14:215–222
DOI 10.1007/s10047-011-0568-6

ORIGINAL ARTICLE

Efficient transfection method using deacylated polyethylenimine-coated magnetic nanoparticles

Daisuke Kami · Shogo Takeda · Hatsune Makino · Masashi Toyoda · Yoko Itakura · Satoshi Gojo · Shunei Kyo · Akihiro Umezawa · Masatoshi Watanabe

Received: 6 October 2010 / Accepted: 31 March 2011 / Published online: 3 May 2011

Abstract Low efficiencies of nonviral gene vectors, such as transfection reagent, limit their utility in gene therapy. To overcome this disadvantage, we report on the preparation and properties of magnetic nanoparticles [diameter (d) = 121.32 ± 27.36 nm] positively charged by cationic polymer deacylated polyethylenimine (PEI max), which boosts gene delivery efficiency compare with polyethylenimine (PEI), and their use for the forced expression of plasmid delivery by application of a magnetic field. Magnetic nanoparticles were coated with PEI max, which enabled their electrostatic interaction with negatively charged molecules such as plasmid. We successfully transfected 81.1 ± 4.0% of the cells using PEI max-coated magnetic nanoparticles (PEI max-nanoparticles). Along with their superior properties as a DNA delivery vehicle, PEI max-nanoparticles offer to deliver various DNA formulations in addition to traditional methods. Furthermore, efficiency of the gene transfer was not inhibited in the presence of serum in the cells. PEI max-nanoparticles may be a promising gene carrier that has high transfection efficiency as well as low cytotoxicity.

Keywords Deacylated polyethylenimine · Magnetic nanoparticle · Efficient nonviral transfection method

D. Kami
Innovative Integration between Medicine and Engineering Based on Information Communications Technology, Yokohama National University Global COE Program, Yokohama, Japan
e-mail: dkami@tmig.or.jp

S. Takeda · M. Watanabe (✉)
Laboratory for Medical Engineering, Division of Materials and Chemical Engineering, Yokohama National University, 79-1 Tokiwadai, Hodogaya-ku, Yokohama 240-8501, Japan
e-mail: mawata@ynu.ac.jp

D. Kami · H. Makino · M. Toyoda · A. Umezawa
Department of Reproductive Biology, National Institute for Child Health and Development, Tokyo, Japan

D. Kami · M. Toyoda (✉) · Y. Itakura · S. Gojo
Vascular Medicine, Research Team for Geriatric Medicine, Tokyo Metropolitan Institute of Gerontology, 35-2 Sakae-cho, Itabashi-ku, Tokyo 173-0015, Japan
e-mail: mtoyoda@tmig.or.jp

S. Gojo · S. Kyo
Division of Therapeutic Strategy for Heart Failure, Department of Cardio-Thoracic Surgery, The University of Tokyo, Tokyo, Japan

Introduction

Nanotechnologies that allow the nondisruptive introduction of carriers in vivo have wide potential for gene and therapeutic delivery systems [1–4]. Extremely small particles have been successfully introduced into living cells without any further modification to enhance endocytic internalization, such as for cationic help. The cells containing the internalized nanoparticles continued to thrive, indicating that the particles have no inhibitory effect on mitosis. Therefore, iron oxide magnetic nanoparticles have played an important role as magnetic resonance imaging contrast agents [5, 6], and cytotoxicity of this nanoparticle was none (or low) [7, 8]. Thereby, the functionalized iron oxide magnetic nanoparticles are expected to be useful as a new gene delivery tool [3].

Cationic polymer polyethylenimine (PEI) (linear, MW 25,000) is known as the transfection reagent in molecular biology [9], and the dispersant in nanotechnology [10]. PEI are configured to form the positively charged complex with DNA, which binds to anionic cell surface residues and

enter the cell via endocytosis [9, 11], keeping the dispersed state in the solution [10]. However, PEI containing residual *N*-acyl groups is a disadvantage for transfection efficiency. Also, the deacylated PEI (PEI max) for transfection reagent was reported, showing an increase in optimal transfection efficiency of 21-fold in comparison with PEI [12].

The transfection method using magnetic nanoparticles utilizes a magnetic force to deliver DNA into target cells. Therefore, the plasmid is first associated with magnetic nanoparticles. Then, the application of a magnetic force drives the plasmid–nanoparticle complexes toward and into the target cells, where the cargo is released (Fig. 1a) [13–16]. The magnetic nanoparticles are also coated with biological polymers, such as PEI, to allow plasmid loading (Fig. 1b). The binding of the negatively charged plasmid to the positively charged PEI max-coated magnetic nanoparticles (PEI max-nanoparticles) occurs relatively quickly. After complex formation, the loaded nanoparticles are incubated together with the target cells on a magnet plate. Owing to the magnetic force, the iron particles are rapidly drawn toward the surface of the cell membrane. Cellular uptake occurs by either endocytosis or pinocytosis [17]. Once delivered to the target cells, the plasmid is released into the cytoplasm [17, 18]. The magnetic nanoparticles accumulate in endosomes and/or vacuoles [18]. Over time, the nanoparticles are degraded and the iron enters normal iron metabolism [19]. An influence of magnetic nanoparticles on cellular functions has not been reported yet. However, in most cases, the increased iron concentration in culture media does not lead to cytotoxic effects [7].

In this study, we coated the transfection reagent, PEI max, on the surface of magnetic nanoparticles and applied a gene vector using PEI max-nanoparticles for a highly efficient transfection method. Our results indicate a high level of expression of the transfected gene in living cells using the plasmid-conjugated PEI max-nanoparticles.

Materials and methods

Materials

Magnetic nanoparticles (γ-Fe_2O_3, $d = 70$ nm) were purchased from CIK NanoTek. PEI max linear (MW 25,000) was purchased from Polysciences Inc. FuGENE HD was purchased from Roche Diagnostics. Deionized water was purchased from Gibco. Magnetic sheet (160 mT), and neodymium magnet (130 mT) was purchased from Magna Co. Ltd.

Preparation of the PEI max-nanoparticles

The magnetic nanoparticles (1.0 g) were dissolved in 30 ml of PEI max solution (1.6 mg PEI max/ml). The mixture was sonicated for 2 min (40 W) on ice, and 20 ml of deionized water was added (final concentration 1.0 mg PEI max/ml). The ferrofluid was centrifuged at 4,100×*g* for 5 min. The supernatant fluids were harvested and transferred into a fresh tube. This fluid was washed twice by deionized water and resolved into an equal volume of the PEI max solution (1.0 mg PEI max/ml). Magnetic nanoparticles in this fluid

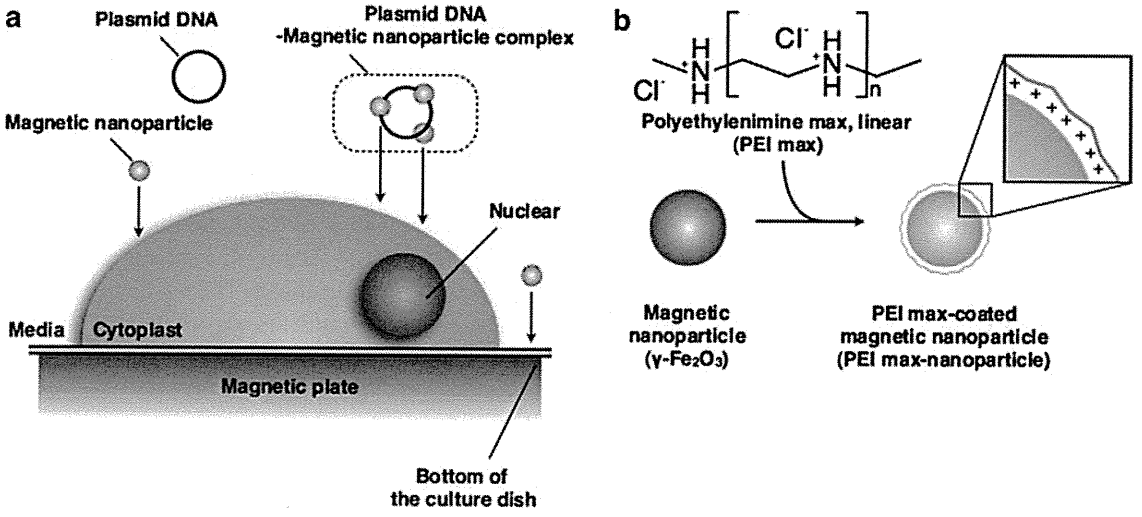

Fig. 1 Nanoparticle transfection method and cationic coating: **a** Plasmid-conjugated magnetic nanoparticles moved to the cell surface on the magnetic sheet upon application of magnetic force. Then, the magnetic force drove this complex toward and into the target cells. **b** Magnetic nanoparticles (γ-Fe_2O_3, $d = 70$ nm) (CIK NanoTek Inc.) were coated with deacylated polyethylenimine max linear (PEI max) (MW 25,000) (Polysciences Inc.), known as a dispersive agent, and transfection reagents. The surface of the PEI max-nanoparticle was positively charged. Nanoparticles and plasmid formed complexes by ionic interaction of the negatively charged plasmid and the positively charged surface of the PEI max-nanoparticle

were coated with PEI max and dispersed in PEI max solution or deionized water.

Measurement of PEI max-nanoparticle size and ζ-potential

The size of the PEI max-nanoparticles was measured with a laser light-scattering method using a fiberoptics particle analyzer (FPAR-1000, Otsuka Electronics). The measurement was performed in triplicate, and median size and range of size distribution were obtained. The ζ-potential of the PEI max-nanoparticles was determined with electrophoretic light-scattering spectrophotometer (ELSZ-2, Otsuka Electronics).

Charge characteristics of PEI max-nanoparticle

PEI max-nanoparticle (100 μg) and each weight of plasmid (2,000, 1,000, 750, 500, 375, 250, 188 ng) were mixed in deionized water or PEI max solution (1 mg/ml). Each solution were reacted for 1 h at room temperature.

Plasmid DNA was bound to PEI max-nanoparticles

Plasmid DNA (5 μg) was reacted with various weights of PEI max-nanoparticles (0–1.8 mg/tube) in deionized water for 15 min at room temperature. Then, the reaction mixtures were centrifuged at 12,000×*g* for 15 min and were formed in a sol-like precipitation in the lower layer. The concentration of DNA in the upper layer (hyaline layer) was determined by NanoDrop 1000 spectrophotometer (Thermo Scientific). The relative concentration of plasmid DNA treated without PEI max-nanoparticles was regarded as 100%.

Cell culture

P19CL6 cells (CL6 cells) from a mouse embryonic carcinoma cell line were grown on 100-mm dishes (Becton-Dickinson) in alpha-minimum essentioal medium (MEM) (Nacalai Tesque) supplemented with 10% fetal bovine serum (FBS) (JRH Bioscience Inc.), penicillin, and streptomycin (Gibco), and were maintained in a 5% carbon dioxide (CO_2) atmosphere at 37°C.

Transfection procedure using PEI max-nanoparticles

CL6 cells were seeded at 1×10^5 cells/well in six-well plates (Becton-Dickinson) 18 h before transfection. Immediately before transfection, cells were rinsed and supplemented with fresh culture medium (1 ml). The PEI max-nanoparticles (in 1 mg PEI max/ml solution) were mixed with 2.0 μg of the plasmid [pCAGGS–enhanced green fluorescent protein (EGFP), the modified pCAGGS expression vector [20], weight ratio PEI max:plasmid = 3:1] and incubated in the deionized water at final volume of 50 μl at room temperature for 15 min. The complexes were added to the CL6 cells on a magnetic sheet various times (0, 0.5, 1, 4, and 24 h). Forty-eight hours after transfection, CL6 cells were evaluated; 1 mg/ml of PEI max solution was used as a positive control.

Quantitative real-time reverse transcriptional (RT)-PCR

Total RNAs from CL6 cells were extracted using ISOGEN (Nippon Gene). To perform quantitative real-time polymerase chain reaction (PCR) assay, total RNA (1 μg) was reverse-transcribed using random hexamer and the PrimeScript RT reagent kit (TaKaRa). Quantitative real-time reverse transcriptional (RT)-PCR was performed on LineGene (BioFlux), using 100 ng of complementary DNA (cDNA) in 25 μl reaction volumes with 10 nmol/l EGFP primer and 12.5 μl of SYBR Premix Ex Taq (TaKaRa). PCR primers for the gene of EGFP and *Gapdh* were designed to amplify each cDNA using the sense primer (5′-CCGACCACATGAAGCAGCAC-3′) and the reverse primer (5′-CTTCAGCTCGATGCGGTTCAC-3′) for the EGFP, and the sense primer (5′-TGCGACTTCAACAGCA ACTC-3′) and the reverse primer (5′-CTTGCTCAGTGTC CTTGCTG-3′) for the *Gapdh*. Calculations were automatically performed by fluorescent quantitative detection system software (BioFlux).

Nanoparticle cytotoxicity

Alamar Blue [21] was used to measure cell proliferation and metabolic activity as an oxidation-reduction indicator. After 48 h of PEI max or PEI max-nanoparticle exposure, 900 μl of medium from each condition was transferred into a 24-well flat-bottomed plate. One hundred microliters of Alamar Blue (AbD Serotec) was added to each well, and the well plate was incubated for 3 h at 37°C. Fluorescence was measured at 570/600 nm in a Viento multispectrophotometer reader (Dainippon Pharmaceutical). The relative absorbance of CL6 cells without any treatment is regarded as 100% (it is indicated as a percent control in Fig. 4c).

Flow cytometric analysis

To count the numbers of EGFP-positive cells using PEI max-nanoparticles (0.8 μg/well in a six-well plate) on a magnetic sheet for 4 h (PEI max alone as a positive control), a Cytomics FC500 (Beckman Coulter Inc.) was used, and data were analyzed with FlowJo Ver.7 (Tree Star Inc.). Each sample was compared with negative control cells (without treatment).

Statistical analysis

Results, shown as the mean ± standard error (SE), were compared by analysis of variance (ANOVA) followed by Scheffe test (http://chiryo.phar.nagoya-cu.ac.jp/javastat/JavaStat-j.htm), with $P < 0.05$ considered significant.

Results

Characterization of PEI max-nanoparticles

Magnetic nanoparticles were well coated with PEI max and were highly dispersed in PEI max solution (1 mg/ml) or deionized water. Secondary size of the PEI max-nanoparticles was approximately 121.32 ± 27.36 nm (Fig. 2A). To evaluate stability in PEI max solution (1 mg/ml) or deionized water, we measured the ζ-potential of PEI max-nanoparticles, which was +45.53 mV in PEI max solution and +30.05 mV in deionized water. The PEI max-nanoparticles were aggregated by magnetic force (Fig. 2Ba) and quickly redispersed by vortex (Fig. 2Bb). Time-lapse photography (30 s/s) shows that magnetic nanoparticles were gradually removed at the site of the neodymium magnet (right side of the tube) for 2 h (magnetic nanoparticles for transfection: http://www.youtube.com/watch?v=Hyjfc4moHK4). These nanoparticles in PEI max solution were not aggregated without magnetic force. To avoid aggregation of plasmid-attached PEI max-nanoparticle caused by charge neutralization, it was necessary that their weight ratio was approximately 1:400 (Fig. 2C). In general, 1–2 μg of plasmid per well was mixed with the transfection reagent such, as PEI max, and FuGENE HD into six-well plates. However, too much (400–800 μg of nanoparticle per well) caused inhibition of transfection (described later). To solve the problem, we decided to use in 1 mg/ml of PEI max solution as a solvent. As a result, each concentration of the plasmid did not aggregate with PEI max-nanoparticle (Fig. 2Bb). To evaluate whether the plasmid DNA was attached to PEI max-nanoparticles in deionized water, we reacted PEI max-nanoparticles with plasmid DNA for 15 min at room temperature. Measuring the concentration of plasmid DNA in the upper layer (hyaline layer), the weight of PEI max-nanoparticles was reduced in a dependent manner (Fig. 2D).

Transfection efficiency using PEI max-nanoparticles and magnetic sheet, and viability of the CL6 cells treated with PEI max-nanoparticles

CL6 cells were transfected with pCAGGS-EGFP and PEI max alone as a positive control (Fig. 3a) and pCAGGS-EGFP and PEI max-nanoparticles (Fig. 3b) at 48 h after transfection. Many EGFP-positive cells were observed among CL6 cells transfected with PEI max-nanoparticles compared with those transfected with PEI max. To evaluate the optimum condition of transfection using PEI max-nanoparticles, quantitative real-time RT-PCR was performed at 48 h after transfection. The optimum condition of transfection was a concentration of 0.8 μg/well (Fig. 4a) on a magnetic sheet for 4 h (Fig. 4b). *EGFP* gene expression level was reduced under transfection of excess magnetic nanoparticles (7.5 μg/well) (Fig. 4a) and prolonged time on the magnetic sheet (24 h) (Fig. 4b). EGFP expression in CL6 cells transfected with PEI max-nanoparticles was increased approximately two to fourfold compared with those transfected with PEI max. The viability of CL6 cells treated with PEI max-nanoparticles, as measured by Alamar Blue assay, did not differ between cells treated with/without PEI max alone (Fig. 4c).

Number of EGFP-positive cells by flow cytometric analysis

Forty-eight hours after transfection using PEI max alone or PEI max-nanoparticles, we examined the number of EGFP-positive cells (total 10,000 cells) by flow cytometric analysis. Compared with the negative control (untreated CL6 cells), 42.2 ± 8.5% of cells treated with PEI max alone (Fig. 5a), 81.1 ± 4.0% of cells treated with 0.8 μg of PEI max-nanoparticles per well on the magnetic sheet for 4 h (Fig. 5b), and 13.9 ± 1.1% of cells treated with FuGENE HD (Fig. 5c) expressed EGFP. The number of EGFP-positive cells was significantly increased (approximately twofold) using PEI max-nanoparticles.

Discussion

In this study, to express target gene with high efficiency and low cytotoxicity, we focused on PEI max and magnetic nanoparticles (γ-Fe_2O_3). Many researchers have reported various transfection methods using PEI and magnetic nanoparticles, such as γ-Fe_2O_3, and superparamagnetic iron oxide nanoparticle (used as magnetic resonance imaging contrast agents) (Table 1). However, these methods had a low transfection efficiency [14, 15], combined with virus (adenovirus, or retrovirus) [15], and high cytotoxicity (low cell viability) [13] and may therefore have little effectiveness for clinical use.

The expression level of the *EGFP* gene was reduced under transfection of excess magnetic nanoparticles (7.5 μg/well) (Fig. 4a). This result may indicate that a high concentration of PEI max-nanoparticles formed the large agglutinate complexes with plasmid DNAs [22, 23]

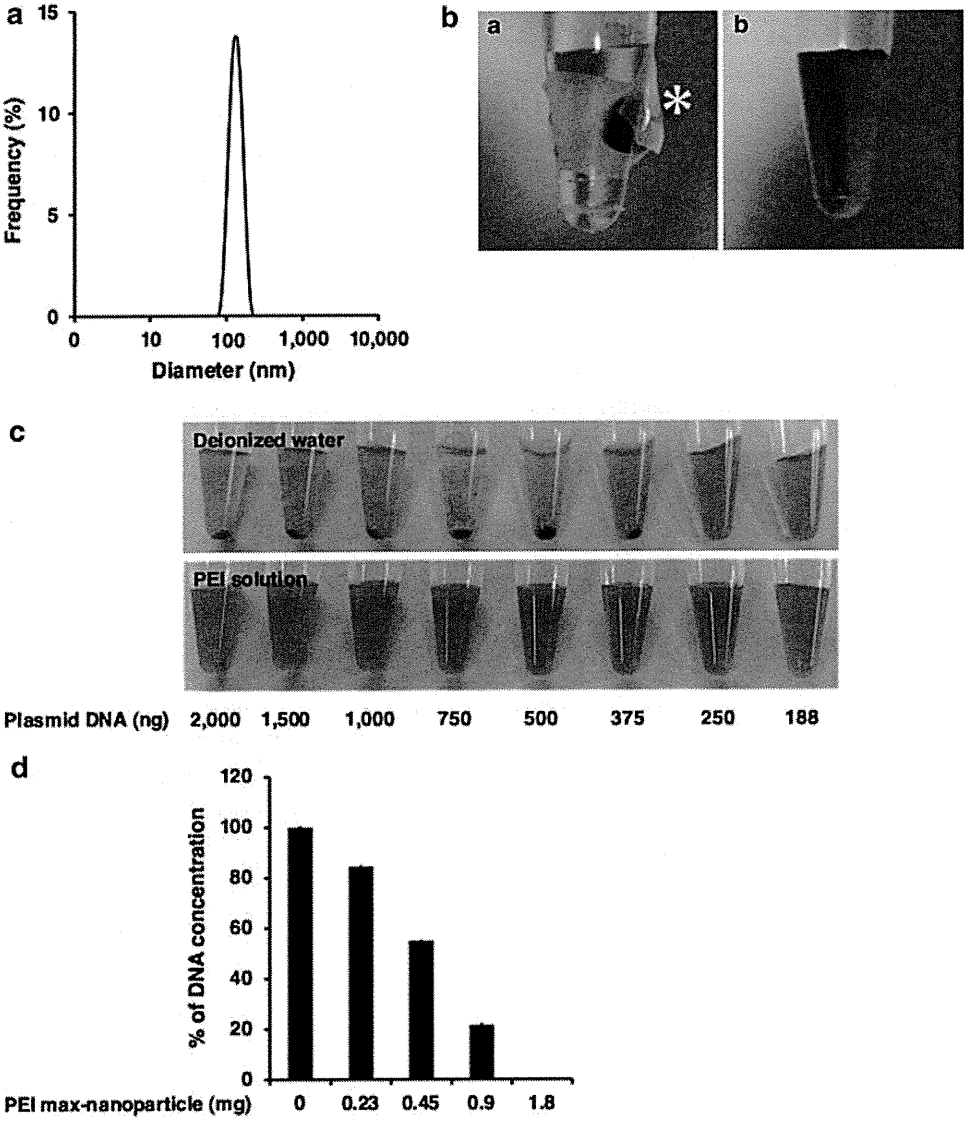

Fig. 2 Characteristics of the deacylated polyethylenimine (PEI max)-nanoparticle: **a** The size of the PEI max-nanoparticles was measured with a laser light-scattering method using a fiberoptics particle analyzer (FPAR-1000, Otsuka Electronics) at 37°C. Secondary particle size of the PEI max-nanoparticles was approximately 121.32 ± 27.36 nm. **b** PEI max-nanoparticles were induced to aggregate by a magnet (*a*) and were then dispersed (*b*). *Asterisk* indicates column-shaped neodymium magnet. **c** Cationic PEI max-nanoparticles (100 μg per tube) in deionized water or PEI max solution (1 mg/ml) were reacted with anionic plasmid [pCAGGS–enhanced green fluorescent protein (EGFP)] by an ionic bond. PEI max-nanoparticles in deionized water and plasmid aggregated more easily than that in PEI max solution and plasmid. **d** To evaluate whether plasmid DNA attached to PEI max-nanoparticles in deionized water, PEI max-nanoparticles were reacted with plasmid DNA for 15 min at room temperature. Measuring the concentration of plasmid DNA in the upper layer (hyaline layer), the weight of PEI max-nanoparticles was reduced in a dependent manner

because PEI max-nanoparticle and plasmid DNA complexes are taken in by endocytosis. Thus, it might be difficult to take the large complexes into the cytoplasm by endocytosis. Furthermore, the expression level of the *EGFP* gene was also reduced under transfection during a prolonged time on the magnetic sheet (24 h) (Fig. 4b). This result may demonstrate a causal relationship between the cell division cycle and time on the magnetic sheet. Plasmid DNAs in the cytoplasm were transported into the nucleus when the nuclear membrane disappeared on cell division [24]. Thus, plasmid DNAs and magnetic nanoparticle complexes might not be transported into the nucleus because they are drawn to the bottom of the cell by magnetic force.

We succeeded in producing PEI max-nanoparticles that enabled P19CL6 cells, which is derived from embryonic carcinoma transfected on a magnetic sheet. In addition, this method resulted in a highly efficient gene transduction compared with that of conventional transfection methods (Fig. 5a, c). This transfection method using PEI max-nanoparticles is a relatively low-cost and quick method of

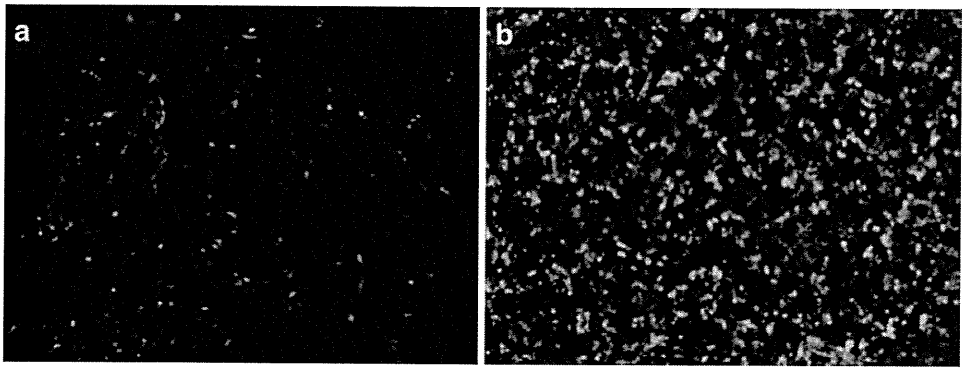

Fig. 3 Enhanced green fluorescent protein (EGFP) expression in CL6 cells using deacylated polyethylenimine (PEI max)-nanoparticle and magnetic field. Phase-contrast fluorescent micrograph of CL6 cells were transfected with pCAGGS-EGFP and PEI max as a control (**a**) and PEI max-nanoparticles (**b**). The numbers of EGFP-positive cells were further increased by PEI max-nanoparticles

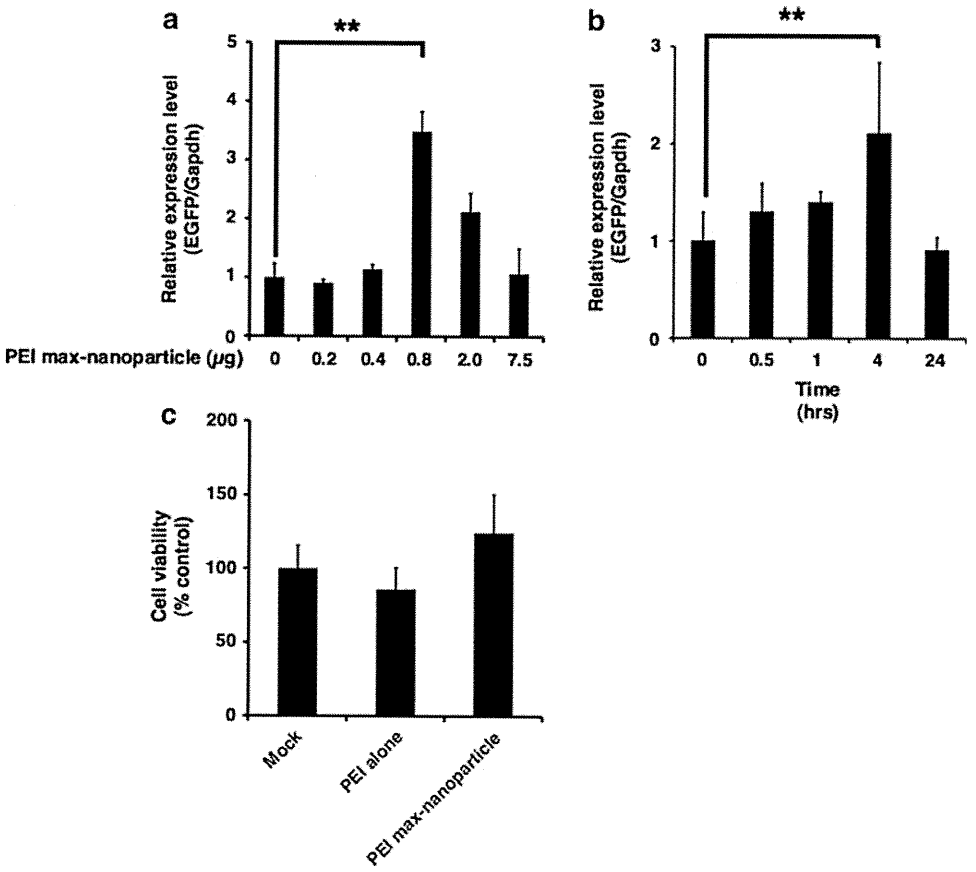

Fig. 4 Optimum condition for transfection of the deacylated polyethylenimine (PEI max)-nanoparticle. To optimize the transfection method, we examined PEI max-nanoparticles in terms of volume (**a**) and time (**b**) on the magnetic sheet. These results were evaluated by quantitative real-time reverse transcriptional polymerase chain reaction (RT-PCR). The expression level of the CL6 cells treated with PEI max alone is regarded as 1. The optimal conditions for transfection using PEI max-nanoparticles were when the CL6 cells were treated with 0.8 μg of PEI max-nanoparticles and 2.0 μg of pCAGGS-EGFP for 4 h on the magnetic sheet. The *double asterisks* indicate a significant difference ($P < 0.05$). Cytotoxicities of PEI max and PEI max-nanoparticles were evaluated by Alamar Blue assay (**c**). After 48 h of PEI max or PEI max-nanoparticle exposure, there were no significant differences in cell viability between CL6 cells treated with PEI max and those with PEI max-nanoparticles. *Mock* the CL6 cells treated without any treatment as a negative control. *PEI max alone* the CL6 cells treated with PEI max. *PEI max-nanoparticles* the CL6 cells treated with PEI max-nanoparticles (0.8 μg) for 4 h on the magnetic sheet. The relative absorbance of untreated CL6 cells is regarded as 100%